

Near-apneic ventilation decreases lung injury and fibroproliferation in an ARDS model with ECMO

Joaquin Araos¹; Leyla Alegria¹; Patricio Garcia²; Pablo Cruces^{4,3}; Dagoberto Soto¹; Benjamín Erranz⁵; Macarena Amthauer¹; Tatiana Salomon⁶; Tania Medina⁷; Felipe Rodriguez¹; Pedro Ayala⁸; Gisella R. Borzone⁸; Manuel Meneses⁹; Felipe Damiani^{1,10}; Jaime Retamal^{1,3}; Rodrigo Cornejo^{11,3}; Guillermo Bugedo^{1,3}; Alejandro Bruhn^{1,3}

¹Departamento de Medicina Intensiva, Facultad de Medicina, Pontificia Universidad Católica de Chile, Santiago, Chile.

²Escuela de Kinesiología, Facultad de Medicina, Pontificia Universidad Católica de Chile, Santiago, Chile.

³Center of Acute Respiratory Critical Illness (ARCI), Santiago, Chile.

⁴Centro de Investigación de Medicina Veterinaria, Escuela de Medicina Veterinaria, Facultad de Ecología y Recursos Naturales, Universidad Andrés Bello, Santiago, Chile.

⁵Centro de Medicina Regenerativa, Facultad de Medicina Clínica Alemana - Universidad del Desarrollo, Santiago, Chile.

⁶Unidad de Pacientes Críticos Pediátrica, Clínica Alemana, Santiago, Chile.

⁷Escuela de Enfermería, Facultad de Medicina, Universidad Finis Terrae, Santiago, Chile.

⁸Departamento de Enfermedades Respiratorias, Facultad de Medicina, Pontificia Universidad Católica de Chile, Santiago, Chile.

⁹Departamento de Anatomía Patológica, Instituto Nacional del Tórax, Santiago, Chile.

¹⁰Escuela de Kinesiología, Facultad de Ciencias, Pontificia Universidad Católica de Valparaíso, Valparaíso, Chile

¹¹Unidad de Pacientes Críticos, Departamento de Medicina, Hospital Clínico Universidad de Chile, Santiago, Chile.

Corresponding author: Alejandro Bruhn, M.D, Ph.D. Departamento de Medicina Intensiva, Edificio Académico Escuela de Medicina, Pontificia Universidad Católica de Chile, Diagonal Paraguay 362, 6° piso, Santiago, Chile. P.O. Box 114D. Email: alejandrob Bruhn@gmail.com

Author contributions: J.A., P.C., J.R., G.B. and A.B. designed the study. J.A., L.A., P.G., P.C., D.S., B.E., M.A., T.S., T.M., F.R., F.D., M.M. and A.B. contributed to data acquisition and analysis. J.A., P.A., G.R.B., M.M., J.R., R.C., G.B. and A.B. contributed to data interpretation. J.A., J.R., R.C., G.B. and A.B. drafted the manuscript, while all other authors revised critically the manuscript for important intellectual content. All authors read and approved the final manuscript.

Funding: P.C., J.R., R.C., G.B. and A.B. acknowledge support from CONICYT through grants Fondecyt # 1130248 and Fondecyt # 1161556. JA acknowledges partial support from CONICYT-Doctorado Nacional/2013. FD acknowledges partial support from CONICYT-PFCHA/Doctorado Nacional/2017-folio 21171551

Short running head: Near-apneic ventilation during ECMO for ARDS

Subject category: 4.7 (Mechanical Ventilation: Applications)

Total word count: 3165 words **At a Glance Commentary**

Scientific Knowledge on the Subject

Approaches to mechanical ventilation during ECMO in ARDS are widely variable. Although lung rest strategies have been proposed, there is scarce evidence to support a recommendation. This is a highly relevant issue since the final impact of ECMO may depend on the possibility of promoting resolution of lung injury.

What This Study Adds to the Field

In this study, in a 24-hour experimental model of severe ARDS supported with ECMO, we compared the use of near-apneic ventilation with a non-protective and with a conventional protective ventilatory strategy. Near-apneic ventilation decreased lung injury compared to the other strategies. In addition, an early fibroproliferative response characterized by extensive staining for myofibroblasts and pro-collagen III, and increased activity of matrix-metalloproteinases 2 and 9, was observed in the lungs of the group ventilated with a non-protective strategy. This response was more consistently decreased by near-apneic ventilation than by a conventional protective ventilation.

This article has an online data supplement, which is accessible from this issue's table of content online at www.atsjournals.org

ABSTRACT

Rationale: There is wide variability in mechanical ventilation settings during ECMO in ARDS patients. Although lung rest is recommended to prevent further injury, there is no evidence to support it.

Objectives: To determine whether near-apneic ventilation decreases lung injury in a pig model of ARDS supported with ECMO.

Methods: Pigs (26-36kg; n=24) were anesthetized and connected to mechanical ventilation. In 18 animals lung injury was induced by a double-hit consisting in repeated saline lavages followed by 2 hours of injurious ventilation. Then, animals were connected to high-flow veno-venous ECMO, and randomized into 3 groups: Non-protective (PEEP 5 cmH₂O, tidal volume 10 ml/kg, respiratory rate 20 bpm); Conventional-protective (PEEP 10 cmH₂O, tidal volume 6 ml/kg, respiratory rate 20 bpm); Near-apneic (PEEP 10 cmH₂O, driving pressure 10 cmH₂O, respiratory rate 5 bpm). Six other pigs were used as Sham. All groups were maintained during the 24-hour study period.

Measurements and Main Results: Minute ventilation and mechanical power were lower in the Near-apneic group, but no differences were observed in oxygenation or compliance. Lung histology revealed less injury in the Near-apneic group. Extensive immunohistochemical staining for myofibroblasts and pro-collagen III was observed in the Non-protective group, with the Near-apneic group exhibiting the least alterations. Near-apneic group showed significantly less matrix-metalloproteinase-2 and -9 activity. Histological lung injury and fibroproliferation scores were positively correlated with driving pressure and mechanical power.

Conclusions: In an ARDS model supported with ECMO, near-apneic ventilation decreased histologic lung injury and matrix-metalloproteinase activity, and prevented the expression of myofibroblast markers.

Abstract word count: 249 words

Keywords: Acute Respiratory Distress Syndrome – Extracorporeal membrane oxygenation
- Ventilator-induced lung injury – Mechanical ventilation - Myofibroblast

INTRODUCTION

Extracorporeal membrane oxygenation (ECMO) is increasingly being used to treat severe acute respiratory distress syndrome (ARDS) patients with refractory hypoxemia (1). Along with improving oxygenation, ECMO enables more protective ventilation by decreasing the intensity of mechanical stimulus on lung tissue.

The concept of resting the lungs with the aid of extracorporeal lung support was first proposed by Gattinoni et al. who applied in a non-controlled series of ARDS patients a low frequency ventilation consisting of respiratory rate below 5 breaths/min (bpm), with a PEEP level ranging from 15 to 25 cmH₂O, and peak inspiratory pressures less than 35–45 cmH₂O, combined with extracorporeal CO₂ removal. They observed a higher survival than expected (2). However, later Morris et al. were unable to demonstrate an advantage of this strategy in a randomized controlled trial. Interestingly, these studies were performed decades ago, well before the development of current understanding of the mechanisms of ventilator-induced lung injury (VILI) (3).

After the landmark studies that have defined the essentials of protective ventilation for ARDS (4-6), recommendations for lung rest during ECMO have also evolved targeting lower driving pressures, but still promoting low respiratory rates. Such a strategy, based mainly on expert opinion, is recommended by the Extracorporeal Life Support Organization (ELSO)(7), and was applied in the CESAR trial to patients connected to ECMO (8). However, recent observational studies and surveys indicate a huge variability in the approach to mechanical ventilation during ECMO for ARDS, and although most physicians support the rationale of resting the lungs (9), most patients are ventilated with

rather conventional ventilatory settings (9, 10). The need for better evidence in this issue has been recently highlighted (11, 12). This factor may be relevant concerning the impact of ECMO on ARDS outcomes. In severe ARDS the remaining aerated lung is usually very small and therefore, conventional protective ventilation with a tidal volume (V_T) of 6 ml/kg may still constitute an excessive mechanical load that can promote further lung injury and even an irreversible fibroproliferative response, counteracting the potential benefits of ECMO.

We hypothesized that in severe acute lung injury the use of near-apneic ventilation, consisting in very low levels of V_T , driving pressure, and respiratory rate, may prevent further damage by minimizing energy transfer to the lungs. The goal of this study was to determine whether a near-apneic ventilatory strategy decreases lung injury and early fibroproliferation, compared to a conventional protective ventilatory strategy, in a severe ARDS model supported with ECMO. Some of the results of this study have been previously reported in the form of an abstract (13).

METHODS

Additional details are available in the online data supplement.

Domestic pigs (28.6 ± 0.4 kg) were treated following recommended guidelines (14). The Institutional Animal Ethics Committee approved the study (Protocol 12-029).

Interventions and study groups

Figure 1 summarizes study design.

a) Preparation: Anesthetic protocol, monitoring, and fluid therapy have been previously described (15). Initially, animals were ventilated using volume controlled ventilation (VCV) with V_T 10 ml/kg, respiratory rate (RR) 16-18 bpm, inspiratory:expiratory time ratio (I:E) 1:2, and PEEP 5 cmH₂O (baseline settings). Inspired O₂ fraction (F_IO₂) was kept at 1.0 during the whole study. After baseline measurements animals were randomly allocated to Sham (n=6) or lung injury (n=18).

b) Induction of lung injury: repeated lung lavages (30 ml/kg warm 0.9% saline solution intratracheally) were performed until PaO₂/FiO₂ was below 250 mmHg, followed by 2 hours of injurious ventilation (pressure controlled ventilation-PCV with PEEP 0 cmH₂O, inspiratory pressure 40 cmH₂O, RR 10 bpm, and I:E 1:1). In parallel, a 23F bi-caval dual lumen cannula (Avalon ELITE®, Maquet, USA) was placed through the jugular vein as previously described (15). Thereafter, ventilation was returned to baseline settings for 10 minutes, time 0 (T₀) measurements were performed, and ECMO started targeting a blood flow > 60 ml/kg/min. Sweep gas flow (FiO₂ 1.0) was initially set 1:1 to blood flow and then titrated to keep PaCO₂ at 40 ± 10 mmHg. At T₀ animals with lung injury were randomly allocated to 3 groups (n=6 per group): *Non-protective*, *Conventional protective*, and *Near-apneic*. *Sham* animals received neither lung injury nor ECMO. Instead, they underwent a 3-hour stabilization period before performing T₀ measurements.

c) Study period: After T₀ measurements animals underwent a 24-hour study period during which they were ventilated as follows:

- Sham and Non-protective groups: VCV with V_T 10 ml/kg, PEEP 5 cmH₂O, RR as baseline, I:E 1:2

- Conventional protective group: VCV with V_T 6 ml/kg, PEEP 10 cmH₂O, RR 20 bpm, I:E 1:2

- Near-apneic group: PCV, PEEP 10 cmH₂O, driving pressure 10 cmH₂O, RR 5 bpm, I:E 1:1.

Data recording and tissue analysis

Respiratory and hemodynamic data were registered at baseline, T₀, and at 3, 12 and 24 hours of the study period (T₃, T₁₂ and T₂₄). At T₂₄ animals were euthanized and the lungs extracted for histology and other tissue analysis.

Semi-quantitative histological scores ranging from 0 (normal) to 3 (severe alteration) were used to evaluate acute lung injury (hematoxylin-eosin), and the presence of alpha-smooth muscle actin (alpha-SMA) and pro-collagen-3 proteins (immunohistochemistry). Real-time PCR was used to measure alpha-SMA, collagens I and III, and transforming growth factor-beta 1 (TGF-β1) mRNA levels. Matrix-metalloproteinases (MMP)-2 and -9 activities were measured using zymography. TGF-β1 protein levels were analyzed by ELISA.

Statistical analysis

Statistical analysis was performed using GraphPad Prism 7. Longitudinal data was analyzed using repeated measures two-way ANOVA, followed by Tukey's multiple comparisons test (16). Single time point data were compared using one-way ANOVA. Linear regression analysis was also performed. Statistical significance was set at $p < 0.05$ and data expressed as mean \pm standard error of the mean.

RESULTS

Respiratory, hemodynamic and biochemical variables

Lung injury led to severe hypoxemia and decreased compliance, without differences between the three injured groups at T_0 (Table 1). Once connected to ECMO oxygenation improved rapidly to $\text{PaO}_2/\text{FiO}_2$ levels above 60 mmHg as a result of extracorporeal gas exchange, but later on $\text{PaO}_2/\text{FiO}_2$ continued to increase throughout the study period reaching $\text{PaO}_2/\text{FiO}_2$ levels above 200 mmHg at T_{24} , without differences between groups. In contrast, compliance remained low at T_{24} in the three groups with lung injury.

During the study period minute ventilation remained unchanged in the Non-protective group, but decreased 30 to 40% in the Conventional protective group, and 10 to 20 times in the Near-apneic group (Table 1). Despite these large differences in minute ventilation, PaCO_2 and pH were not different among groups due to the compensatory modifications made in the sweep gas flow of the ECMO circuit. Other ECMO parameters were similar among groups (Supplementary Table E1).

As a result of the different ventilatory strategies applied to the three groups with lung injury, large differences were observed in two determinants of VILI: driving pressures and mechanical power. Driving pressures remained between 21 and 24 cmH_2O in the Non-protective group, 14 to 15 cmH_2O in the Conventional protective group, and 9 to 10 cmH_2O in the Near-apneic group (Figure 2A). Likewise, mechanical power ranged from 11 to 13 J/min in the Non-protective group, 7 to 8 J/min in the Conventional protective group, and 0.4 to 0.5 J/min in the Near-apneic group, which represents a difference of 10 to 20 fold compared to the other groups (Figure 2B).

The three injured groups exhibited pulmonary hypertension at T_0 , which improved during the study period. Due to hypotension not responding to fluid loading, noradrenaline

infusion was required in the 3 groups with lung injury, with increasing doses throughout the study, and without differences among groups (Table 2).

Analysis of blood biochemical data revealed mild renal and liver dysfunction in the Non-protective group, as indicated by an increase in creatinine and aspartate transaminase (AST) plasma levels (Supplementary Table E2).

Markers of acute lung injury and early fibroproliferative response

Injured animals presented variable degrees of diffuse alveolar damage (Supplementary Figure E1). The severity of injury was lowest in the Near-apneic group, as evidenced by less alveolar disruption, neutrophil infiltration and hemorrhage (Supplementary Table E3), as well as a lower lung injury score than Non-protective and Conventional protective groups (Figure 3). In terms of lung water content, all injured groups had significantly higher wet-dry weight ratios compared to the Sham group, but no differences were observed between them (Figure 4).

Immunohistochemistry staining for alpha-SMA was increased in the Non-protective and Conventional protective groups compared to Sham, but not in the Near-apneic group (Figure 5). Pro-collagen III and TGF- β 1 were increased only in the Non-protective group (Supplementary Figures E2 and E3). MMPs 2 and 9 activities were increased in the three injured groups, but the Near-apneic group had significantly lower levels of activity than Non-protective and Conventional protective groups (Figure 6).

There was an increase in lung tissue mRNA expression of alpha-SMA (> 10 fold) and collagen III (> 1000 fold) expression in all injured groups compared to Sham, but not in

collagen I, nor in TGF- β 1. No differences between the three injured groups were observed (Table 3).

Interestingly, when considering the data of each injured animal individually, we found a positive correlation of histological injury, myofibroblast and pro-collagen III scores, with both, driving pressure and mechanical power (Supplementary Figure E4).

DISCUSSION

The main result of the present study is that in a model of severe ARDS supported with ECMO, 24 hours of non-protective ventilation induces severe lung injury and an early fibroproliferative response, which is more consistently prevented by applying near-apneic ventilation than by just providing conventional protective ventilation.

We designed an experimental study in a model of acute lung injury in pigs supported with ECMO to compare near-apneic ventilation versus a conventional protective ventilatory strategy, in its ability to modulate lung injury. In addition, we included a group ventilated with a non-protective ventilatory strategy, as a positive control to confirm whether the model was sensitive to the influence of the ventilatory strategy. The design was characterized by: high severity of lung injury, to reproduce the clinical context in which ECMO is applied in ARDS patients; a high flow veno-venous ECMO, to allow for effective lung rest; and a prolonged timeframe, to provide enough time for differences to manifest. In a previous report we described how this ARDS model is highly lethal without ECMO due to severe hypoxemia, particularly in the first hours (15).

Ventilatory strategies and acute lung injury

Near-apneic ventilation significantly decreased histologic lung injury compared to both, the non-protective and the conventional protective ventilatory strategies. The three ventilatory strategies applied were associated to marked differences in driving pressures, but also in mechanical power. When looking at individual data, driving pressure and mechanical power were positively correlated with lung injury scores. These two variables have been proposed as predictors of VILI (5, 17). While driving pressure reflects the relation between applied V_T and compliance, mechanical power is a relatively new concept in VILI, aimed at unifying different ventilator parameters into one single, energy input concept, which is influenced not only by V_T , driving pressure and PEEP, but also by flow and respiratory rate. Compared to non-protective and conventional protective ventilatory strategies, near-apneic ventilation decreased driving pressure by 60 and 40 %, respectively. However, the reduction in terms of mechanical power was around ten times. In the study by Cressoni et al. a 12 J/min threshold was established as enough energy to induce whole lung edema in pigs (18). However, those pigs initially had normal lungs. The fact that in our study there was a positive correlation between mechanical power and lung injury, and that animals in the Conventional protective group showed significantly more injury (despite having a mean mechanical power of 7.6 J/min) than those in the Near-apneic group, suggests that mechanical power may be an important factor in the progression of lung damage during severe ARDS and that safe thresholds may depend on the baseline status of the affected lungs.

Interestingly, although the model was characterized by a marked increase in wet-dry weight ratio, this variable was not modulated by the ventilator strategy applied. We speculate that resolution of lung edema may require a longer time frame. Tagami et al. showed that

decreases in extravascular lung water in ARDS patients that survived were only evident after 48 hours of evolution (19).

The very low respiratory rate (RR) contributed significantly to the marked decrease in mechanical power observed in the Near-apneic group. Previous experimental studies have shown that decreasing RR may prevent VILI (20, 21). Furthermore, lung rest strategies proposed for ARDS patients on ECMO consistently include RRs of 5 to 10 bpm (7, 8). Accordingly, we decided to set RR at 5 bpm in the near-apneic group. In contrast, more conservative approaches to mechanical ventilation during ECMO usually apply RRs rather similar to those applied during conventional protective ventilation for ARDS. Schmidt et al. reported that RRs applied the first day after connection to ECMO in 168 ARDS patients ranged from 10 to 25 bpm (10). Similarly, in the recently published EOLIA trial, after connection to ECMO patients were ventilated with a mean RR of 23 bpm (22). Therefore, to reflect this strategy we set RR at 20 bpm in the Conventional protective group. However, from the present study we can't define the relative contribution of decreasing RR versus decreasing V_T , in the benefits observed in the Near-apneic group.

In a study using a postpneumectomy ARDS model in pigs, Iglesias et al. showed that near-apneic ventilation associated to extracorporeal CO_2 removal decreased lung injury, compared to a conventional protective ventilatory strategy. In that model standard protective ventilation with V_T 6 ml/kg was associated to driving pressures above 20 cmH₂O, which decreased to less than 5 cmH₂O in the near-apneic strategy (23). In a randomized controlled trial in 79 patients with moderate to severe ARDS, Bein et al. studied the effect of decreasing V_T to 3 ml/kg with the aid of extracorporeal CO_2 removal, compared to conventional treatment with V_T of 6 ml/kg. In the treated arm driving pressure

could be decreased from 13 to 8 cmH₂O, and there was a decrease in serum IL-6 concentrations in plasma, but there were no differences in any clinical outcome. In this study patients ventilated with conventional treatment were not exposed to high driving pressures, which may explain the negative result of the trial. In fact, a post hoc analysis showed that in the subgroup of patients with more severe ARDS there was a significant increase in ventilator-free days in the treated group (24). Unfortunately, mechanical power calculations can't be extracted from the available data of these studies. Nevertheless, our data suggests that the rationale for setting mechanical ventilation during ECMO should take into account mechanical predictors of VILI such as driving pressure and mechanical power. A recent observational study in patients with severe ARDS supported by ECMO showed that maintaining low driving pressures during the first days is associated with lower mortality (25).

Early fibroproliferative response

In our 24-hour model we found consistent evidence of an early fibroproliferative response, as indicated by the strong presence of myofibroblasts and pro-collagen III in alveolar walls, increased concentrations of TGF- β 1 in lung tissue, increased mRNA expression of collagen III and alpha-SMA, and increased activity of MMPs 2 and 9. Moreover, these markers of fibroproliferation were modulated by the ventilatory strategy applied, with near-apneic ventilation exhibiting the least alterations. Other studies had previously observed evidence of early fibroproliferation in acute lung injury models (26).

Several authors have implicated VILI in the etiology of ARDS-associated fibrosis (27, 28). Although the incidence of fibrosis seems to have dropped with the implementation of protective ventilation (29), recent studies suggest that it still represents a potential and

serious complication of ARDS (30). Bhattacharya and Matthay suggested that ECMO support might be helpful to rest the lungs in order to facilitate lung repair by using low- to very-low V_T (27). Physiologic lung repair is a delicate process that can turn into pathologic and lead to irreversible fibrosis in ARDS patients by different stimuli (28). Pathologic extracellular matrix formation, including inhibition of myofibroblast apoptosis and increased synthesis of pro-collagen 3, have been described in the presence of abnormally high mechanotransduction (31), which in the face of highly inhomogenous ARDS lungs, may occur even when using conventional low V_T ventilation. In fact, although in our study the staining for myofibroblasts and pro-collagen 3 was particularly high in the Non-protective group, we observed a positive and significant correlation of myofibroblast and pro-collagen 3 scores with both driving pressure and mechanical power. MMPs have also been shown to be involved in the pathogenesis of ARDS and VILI (32, 33), and near-apneic ventilation decreased MMP activity compared to the other strategies. These observations suggest that decreasing strain and energy applied to lungs of ARDS patients, by combining ECMO with near-apneic ventilation, may help preventing a fibroproliferative phenotype.

It is important to acknowledge that the early fibroproliferative response observed could represent either a normal repair process after lung injury, or an abnormal fibroproliferation that ultimately ends in fibrosis. Future studies evaluating the long-term impact of this early fibroproliferative response are warranted. Persistence of excessive mechanotransduction is key in perpetuating pathologic fibroproliferation (31), which may explain the lower fibroproliferation observed in the Near-apneic group.

Limitations

We must acknowledge that our study has several limitations. The model applied reproduces the main clinical features of ARDS, but may differ from human ARDS in several pathophysiologic aspects. Other limitation is that we used a FiO_2 of 1.0 throughout the study. Although this deviates from clinical practice and may contribute to lung injury, in pilot experiments we realized that many animals were unable to keep PaO_2 above 60 mmHg, despite maximal ECMO support, unless a high FiO_2 was applied for mechanical ventilation. Pigs have a higher metabolism than humans and this may explain why extracorporeal O_2 transfer alone was insufficient to match metabolic O_2 consumption. In addition, we did not want to modify FiO_2 throughout the study to avoid new covariates that could influence final results. But of course a FiO_2 of 1.0 should not be part of a lung rest strategy during ECMO in patients. Finally, as the different strategies applied differed in several ventilatory parameters, we can't define the relative contribution of each parameter to the results observed.

Clinical implications

The results of this study highlight the relevance of optimizing mechanical ventilation in ARDS patients connected to ECMO. In the most severe cases, such as those patients with very low compliance, such optimization may require decreasing the intensity of mechanical ventilation well beyond conventional ventilatory settings, in order to prevent further lung injury. However, caution is needed in extrapolating these results to clinical practice, as this approach may conflict with other relevant goals, such as decreasing sedatives or allowing spontaneous breathing efforts. Therefore, controlled clinical studies are required to determine the impact of near-apneic ventilation on clinically relevant outcomes.

Conclusions

In an experimental model of severe ARDS supported with ECMO, near-apneic ventilation induced less histologic lung injury and MMP activity than non-protective and conventional protective ventilatory strategies. In addition, near-apneic ventilation prevented the expression of myofibroblast markers, which was observed in the groups ventilated with non-protective and conventional protective strategies.

ACKNOWLEDGEMENTS

We are very thankful to Gabriel Castro for his assistance in the care of animals and the ECMO circuits. In addition, we thank Diego Romero for his valuable help in preparing lung tissue for histologic analysis. Finally, we thank Carlos Martinez for his support in placing vascular access and the ECMO cannulas.

REFERENCES

1. Ventetuolo CE, Muratore CS. Extracorporeal life support in critically ill adults. *Am J Respir Crit Care Med* 2014; 190: 497-508.
2. Gattinoni L, Pesenti A, Mascheroni D, Marcolin R, Fumagalli R, Rossi F, Iapichino G, Romagnoli G, Uziel L, Agostoni A, et al. Low-frequency positive-pressure ventilation with extracorporeal CO₂ removal in severe acute respiratory failure. *JAMA* 1986; 256: 881-886.
3. Morris AH, Wallace CJ, Menlove RL, Clemmer TP, Orme JF, Jr., Weaver LK, Dean NC, Thomas F, East TD, Pace NL, Suchyta MR, Beck E, Bombino M, Sittig DF, Bohm S, Hoffmann B, Becks H, Butler S, Pearl J, Rasmusson B. Randomized clinical trial of pressure-controlled inverse ratio ventilation and extracorporeal CO₂ removal for adult respiratory distress syndrome. *Am J Respir Crit Care Med* 1994; 149: 295-305.
4. Acute Respiratory Distress Syndrome N, Brower RG, Matthay MA, Morris A, Schoenfeld D, Thompson BT, Wheeler A. Ventilation with lower tidal volumes as compared with traditional tidal volumes for acute lung injury and the acute respiratory distress syndrome. *N Engl J Med* 2000; 342: 1301-1308.

5. Amato MB, Meade MO, Slutsky AS, Brochard L, Costa EL, Schoenfeld DA, Stewart TE, Briel M, Talmor D, Mercat A, Richard JC, Carvalho CR, Brower RG. Driving pressure and survival in the acute respiratory distress syndrome. *N Engl J Med* 2015; 372: 747-755.
6. Brower RG, Lanken PN, MacIntyre N, Matthay MA, Morris A, Ancukiewicz M, Schoenfeld D, Thompson BT, National Heart L, Blood Institute ACTN. Higher versus lower positive end-expiratory pressures in patients with the acute respiratory distress syndrome. *N Engl J Med* 2004; 351: 327-336.
7. ELSO Guidelines for Cardiopulmonary Extracorporeal Life Support. Extracorporeal Life Support Organization, Version 1.4 August 2017 [accessed 2018 Apr 16]. Available from: <http://www.else.org>.
8. Peek GJ, Mugford M, Tiruvoipati R, Wilson A, Allen E, Thalanany MM, Hibbert CL, Truesdale A, Clemens F, Cooper N, Firmin RK, Elbourne D. Efficacy and economic assessment of conventional ventilatory support versus extracorporeal membrane oxygenation for severe adult respiratory failure (CESAR): a multicentre randomised controlled trial. *Lancet* 2009; 374: 1351-1363.
9. Marhong JD, Telesnicki T, Munshi L, Del Sorbo L, Detsky M, Fan E. Mechanical ventilation during extracorporeal membrane oxygenation. An international survey. *Ann Am Thorac Soc* 2014; 11: 956-961.
10. Schmidt M, Stewart C, Bailey M, Nieszkowska A, Kelly J, Murphy L, Pilcher D, Cooper DJ, Scheinkestel C, Pellegrino V, Forrest P, Combes A, Hodgson C. Mechanical ventilation management during extracorporeal membrane oxygenation for acute respiratory distress syndrome: a retrospective international multicenter study. *Crit Care Med* 2015; 43: 654-664.

11. Marhong JD, Munshi L, Detsky M, Telesnicki T, Fan E. Mechanical ventilation during extracorporeal life support (ECLS): a systematic review. *Intensive Care Med* 2015; 41: 994-1003.
12. Schmidt M, Pellegrino V, Combes A, Scheinkestel C, Cooper DJ, Hodgson C. Mechanical ventilation during extracorporeal membrane oxygenation. *Crit Care* 2014; 18: 203.
13. Araos J, Cruces P, Tapia P, Alegria L, García P, Salomon T, Rodriguez F, Amthauer M, Castro G, Erranz B, Soto D, Carreño P, Medina T, Damiani F, Bugedo G, Bruhn A. Effect of a Lung Rest Strategy During Ecmo in a Porcine Acute Lung Injury Model. *Intensive Care Medicine Experimental* 2015; 3: A503.
14. Council NR. Guide for the Care and Use of Laboratory Animals: Eighth Edition. Washington, DC: The National Academies Press; 2011.
15. Araos J, Alegria L, Garcia P, Damiani F, Tapia P, Soto D, Salomon T, Rodriguez F, Amthauer M, Erranz B, Castro G, Carreno P, Medina T, Retamal J, Cruces P, Bugedo G, Bruhn A. Extracorporeal membrane oxygenation improves survival in a novel 24-hour pig model of severe acute respiratory distress syndrome. *Am J Transl Res* 2016; 8: 2826-2837.
16. Morais CCA, Koyama Y, Yoshida T, Plens GM, Gomes S, Lima CAS, Ramos OPS, Pereira SM, Kawaguchi N, Yamamoto H, Uchiyama A, Borges JB, Vidal Melo MF, Tucci MR, Amato MBP, Kavanagh BP, Costa ELV, Fujino Y. High Positive End-Expiratory Pressure Renders Spontaneous Effort Noninjurious. *Am J Respir Crit Care Med* 2018; 197: 1285-1296.
17. Gattinoni L, Tonetti T, Cressoni M, Cadringer P, Herrmann P, Moerer O, Protti A, Gotti M, Chiurazzi C, Carlesso E, Chiumello D, Quintel M. Ventilator-related

- causes of lung injury: the mechanical power. *Intensive Care Med* 2016; 42: 1567-1575.
18. Cressoni M, Gotti M, Chiurazzi C, Massari D, Algieri I, Amini M, Cammaroto A, Brioni M, Montaruli C, Nikolla K, Guanziroli M, Dondossola D, Gatti S, Valerio V, Vergani GL, Pugin P, Cadringer P, Gagliano N, Gattinoni L. Mechanical Power and Development of Ventilator-induced Lung Injury. *Anesthesiology* 2016; 124: 1100-1108.
 19. Tagami T, Nakamura T, Kushimoto S, Tosa R, Watanabe A, Kaneko T, Fukushima H, Rinka H, Kudo D, Uzu H, Murai A, Takatori M, Izumino H, Kase Y, Seo R, Takahashi H, Kitazawa Y, Yamaguchi J, Sugita M, Takahashi H, Kuroki Y, Kanemura T, Morisawa K, Saito N, Irahara T, Yokota H. Early-phase changes of extravascular lung water index as a prognostic indicator in acute respiratory distress syndrome patients. *Ann Intensive Care* 2014; 4: 27.
 20. Hotchkiss JR, Jr., Blanch L, Murias G, Adams AB, Olson DA, Wangenstein OD, Leo PH, Marini JJ. Effects of decreased respiratory frequency on ventilator-induced lung injury. *Am J Respir Crit Care Med* 2000; 161: 463-468.
 21. Retamal J, Borges JB, Bruhn A, Cao X, Feinstein R, Hedenstierna G, Johansson S, Suarez-Sipmann F, Larsson A. High respiratory rate is associated with early reduction of lung edema clearance in an experimental model of ARDS. *Acta Anaesthesiol Scand* 2016; 60: 79-92.
 22. Combes A, Hajage D, Capellier G, Demoule A, Lavoue S, Guervilly C, Da Silva D, Zafrani L, Tirot P, Veber B, Maury E, Levy B, Cohen Y, Richard C, Kalfon P, Bouadma L, Mehdaoui H, Beduneau G, Lebreton G, Brochard L, Ferguson ND, Fan E, Slutsky AS, Brodie D, Mercat A, Eolia Trial Group R, Ecmonet. Extracorporeal

- Membrane Oxygenation for Severe Acute Respiratory Distress Syndrome. *N Engl J Med* 2018; 378: 1965-1975.
23. Iglesias M, Jungebluth P, Petit C, Matute MP, Rovira I, Martinez E, Catalan M, Ramirez J, Macchiarini P. Extracorporeal lung membrane provides better lung protection than conventional treatment for severe postpneumectomy noncardiogenic acute respiratory distress syndrome. *J Thorac Cardiovasc Surg* 2008; 135: 1362-1371.
24. Bein T, Weber-Carstens S, Goldmann A, Muller T, Staudinger T, Brederlau J, Muellenbach R, Dembinski R, Graf BM, Wewalka M, Philipp A, Wernecke KD, Lubnow M, Slutsky AS. Lower tidal volume strategy (approximately 3 ml/kg) combined with extracorporeal CO₂ removal versus 'conventional' protective ventilation (6 ml/kg) in severe ARDS: the prospective randomized Xtravent-study. *Intensive Care Med* 2013; 39: 847-856.
25. Serpa Neto A, Schmidt M, Azevedo LC, Bein T, Brochard L, Beutel G, Combes A, Costa EL, Hodgson C, Lindskov C, Lubnow M, Lueck C, Michaels AJ, Paiva JA, Park M, Pesenti A, Pham T, Quintel M, Marco Ranieri V, Ried M, Roncon-Albuquerque R, Jr., Slutsky AS, Takeda S, Terragni PP, Vejen M, Weber-Carstens S, Welte T, Gama de Abreu M, Pelosi P, Schultz MJ, Re VARN, the PNI. Associations between ventilator settings during extracorporeal membrane oxygenation for refractory hypoxemia and outcome in patients with acute respiratory distress syndrome: a pooled individual patient data analysis : Mechanical ventilation during ECMO. *Intensive Care Med* 2016; 42: 1672-1684.
26. Curley GF, Contreras M, Higgins B, O'Kane C, McAuley DF, O'Toole D, Laffey JG. Evolution of the inflammatory and fibroproliferative responses during resolution

- and repair after ventilator-induced lung injury in the rat. *Anesthesiology* 2011; 115: 1022-1032.
27. Bhattacharya J, Matthay MA. Regulation and repair of the alveolar-capillary barrier in acute lung injury. *Annu Rev Physiol* 2013; 75: 593-615.
28. Cabrera-Benitez NE, Laffey JG, Parotto M, Spieth PM, Villar J, Zhang H, Slutsky AS. Mechanical ventilation-associated lung fibrosis in acute respiratory distress syndrome: a significant contributor to poor outcome. *Anesthesiology* 2014; 121: 189-198.
29. Hendrickson CM, Crestani B, Matthay MA. Biology and pathology of fibroproliferation following the acute respiratory distress syndrome. *Intensive Care Med* 2015; 41: 147-150.
30. Forel JM, Guervilly C, Hraiech S, Voillet F, Thomas G, Somma C, Secq V, Farnarier C, Payan MJ, Donati SY, Perrin G, Trousse D, Dizier S, Chiche L, Baumstarck K, Roch A, Papazian L. Type III procollagen is a reliable marker of ARDS-associated lung fibroproliferation. *Intensive Care Med* 2015; 41: 1-11.
31. Hinz B. Formation and function of the myofibroblast during tissue repair. *J Invest Dermatol* 2007; 127: 526-537.
32. Foda HD, Rollo EE, Drews M, Conner C, Appelt K, Shalinsky DR, Zucker S. Ventilator-induced lung injury upregulates and activates gelatinases and EMMPRIN: attenuation by the synthetic matrix metalloproteinase inhibitor, Prinomastat (AG3340). *Am J Respir Cell Mol Biol* 2001; 25: 717-724.
33. Ricou B, Nicod L, Lacraz S, Welgus HG, Suter PM, Dayer JM. Matrix metalloproteinases and TIMP in acute respiratory distress syndrome. *Am J Respir Crit Care Med* 1996; 154: 346-352.

FIGURE LEGENDS

Figure 1. Study design and timeline. Preparation corresponds to anesthesia and invasive monitoring, which took 1-1.5 hours. Lung injury corresponds to the induction of lung injury by 2 hits: repeated saline lavages (1-1.5 hours) followed by 2 hours of injurious ventilation. T_0 to T_{24} corresponds to the study period, during which each group received a specific ventilatory strategy. Abbreviations: V_T = tidal volume in ml/kg, PEEP = positive end-expiratory pressure in cmH₂O, RR = respiratory rate in breaths/min, ECMO = extracorporeal membrane oxygenation, ΔP = driving pressure in cmH₂O.

Figure 2. Determinants of VILI. Panel A: Driving pressure, calculated as plateau pressure – PEEP, at different time points for each study group. **Panel B:** Mechanical power, calculated according to Gattinoni et al. (Ref. 17), at different time points for each study group.

* $p < 0.05$ compared to Sham from T_3 to T_{24} , † $p < 0.05$ compared to Non-protective from T_3 to T_{24} , ‡ $p < 0.05$ compared to Conventional protective from T_3 to T_{24} . Only statistical differences between groups are marked.

Figure 3. Histological assessment of lung injury. Panel A: Representative images of lung histology for each study group (original magnification: 200x, hematoxylin and eosin). Images from Non-protective and Conventional protective groups presented diffuse alveolar damage with alveolar edema, hemorrhage, hyaline membranes and inflammatory cells in the interstitium and alveolar spaces; **Panel B:** Quantitative score for lung injury (from 0 = normal, to 3 = maximal alteration), calculated by averaging the scores for alveolar

disruption, neutrophil infiltration, and hemorrhage, for dependent and non-dependent areas of the right lung, and the global score (mean of scores for dependent and non-dependent areas).

* $p < 0.05$ compared to Sham; † $p < 0.05$ for differences with Non-protective, ‡ $p < 0.05$ for differences with Conventional protective.

Figure 4. Wet-dry lung weight ratio. Wet-dry weight ratio of dependent and non-dependent areas of the left lung. Global columns correspond to the average of the dependent and non-dependent areas. All injured groups showed a significant increase in their lung water content compared to Sham but no differences were detected between them.

* $p < 0.05$ compared to Sham.

Figure 5. Immunohistochemistry of alpha-SMA. Immunohistochemical staining of alpha-SMA protein as a surrogate for myofibroblasts in lung tissue preparations. **Panel A:** Representative images for each study group. Brown staining shows a positive reaction for alpha-SMA (original magnification 400x). In the image corresponding to a Sham animal, alpha-SMA staining is limited to the bronchial wall, which usually has a smooth muscle layer. In contrast, the animal from the Non-protective group has extensive staining on its alveolar walls, while the animal from the Conventional protective group exhibits a moderate staining. **Panel B:** Quantitative score for myofibroblast staining (from 0 = no staining, to 3 = maximal staining) for dependent and non-dependent areas of the right lung, and the global score (mean of scores for dependent and non-dependent areas). Staining in bronchial and vascular walls was not considered for scoring.

* $p < 0.05$ compared to Sham; † $p < 0.05$ for differences with Non-protective.

Figure 6. Matrix-metalloproteinase (MMP)-9 and -2 activities in lung tissue.

Quantitative analysis of gelatin zymography performed in homogenates of the left lung. Data is expressed in arbitrary units (AU) of the 90 kDa band, corresponding to the activity of MMP-9 (left), and of the sum of the 68 and 72 kDa bands, corresponding to the activity of MMP-2 (right).

* $p < 0.05$ compared to Sham; † $p < 0.05$ for differences with Non-protective, ‡ $p < 0.05$ for differences with Conventional protective.

TABLES

Table 1. Respiratory variables

Variable	Group			
	Sham	Non-protective	Conventional protective	Near-apneic
PaO₂/FiO₂ (mmHg)				
<i>Baseline</i>	356 ± 83	353 ± 23	442 ± 23	384 ± 59
<i>T₀</i>	372 ± 24	78 ± 22 ^{*§}	55 ± 10 ^{*§}	56 ± 8 ^{*§}
<i>T₃</i>	348 ± 20	148 ± 20 [*]	168 ± 19 ^{*ll}	101 ± 18 [*]
<i>T₁₂</i>	388 ± 33	233 ± 34 ^{*ll}	300 ± 26	237 ± 28 ^{*ll}
<i>T₂₄</i>	375 ± 28	259 ± 25 ^{*ll}	256 ± 35	300 ± 31 ^{*ll}
PaCO₂ (mmHg)				
<i>Baseline</i>	37 ± 2	42 ± 2	35 ± 2	42 ± 3
<i>T₀</i>	37 ± 2	36 ± 3	30 ± 2	38 ± 4
<i>T₃</i>	41 ± 1	35 ± 1	38 ± 3 ^{ll}	45 ± 5
<i>T₁₂</i>	44 ± 3	34 ± 0	45 ± 2 ^{†ll}	45 ± 4 ^{†ll}
<i>T₂₄</i>	37 ± 3	36 ± 2	41 ± 3 ^{ll}	45 ± 6
PmvO₂ (mmHg)				
<i>T₀</i>	n.d	44 ± 6	28 ± 2	30 ± 1
<i>T₂₄</i>	n.d	85 ± 8 ^{ll}	92 ± 10 ^{ll}	78 ± 4 ^{ll}
Respiratory rate (breaths/min)				
<i>Baseline</i>	18 ± 0	20 ± 1	20 ± 1	19 ± 1
<i>T₀</i>	18 ± 0	19 ± 1	18 ± 1	19 ± 1

T_3	18 ± 0	20 ± 0	19 ± 1	$5 \pm 0^{*\dagger\ddagger\parallel}$
T_{12}	19 ± 1	20 ± 0	$20 \pm 0^{\parallel}$	$5 \pm 0^{*\dagger\ddagger\parallel}$
T_{24}	20 ± 0	20 ± 0	$20 \pm 0^{\parallel}$	$5 \pm 0^{*\dagger\ddagger\parallel}$
Tidal volume (ml/kg)				
<i>Baseline</i>	10.1 ± 0.1	10.2 ± 0.1	9.8 ± 0.3	9.8 ± 0.4
T_0	10.1 ± 0.1	10.2 ± 0.1	9.8 ± 0.3	9.8 ± 0.4
T_3	10.4 ± 0.3	10.1 ± 0.4	$5.9 \pm 0.3^{*\dagger\parallel}$	$2.0 \pm 0.2^{*\dagger\ddagger\parallel}$
T_{12}	10.2 ± 0.3	$9.3 \pm 0.4^{\parallel}$	$5.9 \pm 0.3^{*\dagger\parallel}$	$2.1 \pm 0.1^{*\dagger\ddagger\parallel}$
T_{24}	10.1 ± 0.3	10.1 ± 0.1	$6.0 \pm 0.2^{*\dagger\parallel}$	$2.1 \pm 0.2^{*\dagger\ddagger\parallel}$
Minute ventilation (L/min)				
<i>Baseline</i>	5.2 ± 0.2	5.9 ± 0.3	5.4 ± 0.1	5.2 ± 0.3
T_0	5.4 ± 0.3	5.4 ± 0.2	5.1 ± 0.2	5.3 ± 0.3
T_3	5.4 ± 0.2	5.8 ± 0.2	$3.2 \pm 0.1^{*\dagger\parallel}$	$0.3 \pm 0.0^{*\dagger\ddagger\parallel}$
T_{12}	5.4 ± 0.3	5.3 ± 0.2	$3.3 \pm 0.1^{*\dagger\parallel}$	$0.3 \pm 0.0^{*\dagger\ddagger\parallel}$
T_{24}	5.5 ± 0.3	5.8 ± 0.1	$3.4 \pm 0.0^{*\dagger\parallel}$	$0.3 \pm 0.0^{*\dagger\ddagger\parallel}$
Plateau pressure (cmH₂O)				
<i>Baseline</i>	13 ± 0	14 ± 1	14 ± 0	14 ± 0
T_0	13 ± 0	$22 \pm 1^{*\S}$	$21 \pm 1^{*\S}$	$24 \pm 1^{*\S}$
T_3	13 ± 1	$29 \pm 1^{*\parallel}$	$25 \pm 2^{*\parallel}$	$20 \pm 0^{*\dagger\ddagger\parallel}$
T_{12}	14 ± 1	$28 \pm 1^{*\parallel}$	$25 \pm 2^{*\parallel}$	$20 \pm 0^{*\dagger\ddagger\parallel}$
T_{24}	15 ± 1	$26 \pm 1^{*\parallel}$	$24 \pm 2^{*\parallel}$	$19 \pm 0^{*\dagger\ddagger\parallel}$
PEEP (cmH₂O)				
<i>Baseline</i>	5 ± 0	5 ± 0	5 ± 0	5 ± 0

T_0	5 ± 0	5 ± 0	5 ± 0	5 ± 0
T_3	5 ± 0	5 ± 0	$10 \pm 0^{*\dagger\parallel}$	$10 \pm 0^{*\dagger\parallel}$
T_{12}	5 ± 0	5 ± 0	$10 \pm 0^{*\dagger\parallel}$	$10 \pm 0^{*\dagger\parallel}$
T_{24}	5 ± 0	5 ± 0	$10 \pm 0^{*\dagger\parallel}$	$10 \pm 0^{*\dagger\parallel}$
RS static compliance (ml/cmH₂O)				
<i>Baseline</i>	35 ± 2	35 ± 3	31 ± 2	32 ± 1
T_0	37 ± 2	$17 \pm 1^{*\S}$	$19 \pm 2^{*\S}$	$15 \pm 1^{*\S}$
T_3	36 ± 5	$13 \pm 0.6^*$	$12 \pm 2^*$	$7 \pm 1^{\parallel}$
T_{12}	35 ± 4	$12 \pm 0.4^*$	$12 \pm 1^{\parallel}$	$7 \pm 1^{\parallel}$
T_{24}	32 ± 4	$15 \pm 1^*$	$13 \pm 1^*$	$7 \pm 2^{\parallel}$

Abbreviations: PaO₂/FiO₂: partial pressure of arterial O₂ to fraction of inspired O₂ ratio; PaCO₂: partial pressure of arterial CO₂; PmvO₂: partial pressure of mixed venous O₂; PEEP: positive end-expiratory pressure; RS: respiratory system; n.d.: not determined.

* p < 0.05 compared to Sham, † p < 0.05 compared to Non-protective, ‡ p < 0.05 compared to Conventional protective. All time points were compared to T₀. § p < 0.05 for T₀ compared to baseline, ‖ p < 0.05 compared to T₀.

Table 2. Hemodynamic variables

Variable	Group			
	Sham	Non-protective	Conventional protective	Near-apneic
Heart rate (beats/min)				
<i>Baseline</i>	95 ± 6	65 ± 9	71 ± 5	82 ± 5
<i>T₀</i>	79 ± 5	91 ± 7	74 ± 8	96 ± 6
<i>T₃</i>	68 ± 8	124 ± 5 ^{*II}	130 ± 16 ^{*II}	130 ± 11 ^{*II}
<i>T₁₂</i>	98 ± 4	121 ± 5 ^{*II}	124 ± 6 ^{*II}	122 ± 7 ^{*II}
<i>T₂₄</i>	97 ± 2	110 ± 5	111 ± 9 ^{II}	120 ± 3 ^{II}
MAP (mmHg)				
<i>Baseline</i>	100 ± 6	102 ± 7	85 ± 9	88 ± 5
<i>T₀</i>	102 ± 4	103 ± 8	76 ± 2 [*]	87 ± 4
<i>T₃</i>	92 ± 5	78 ± 6 ^{II}	75 ± 6	73 ± 3
<i>T₁₂</i>	83 ± 7	73 ± 3 ^{II}	77 ± 5	69 ± 2
<i>T₂₄</i>	72 ± 4 ^{II}	77 ± 6 ^{II}	69 ± 4	67 ± 4
mPAP (mmHg)				
<i>Baseline</i>	21 ± 1	22 ± 1	18 ± 1	18 ± 1
<i>T₀</i>	21 ± 1 [§]	39 ± 1 ^{*§}	27 ± 2 ^{*†§}	41 ± 4 ^{*§‡}
<i>T₃</i>	20 ± 1	28 ± 1 ^{*II}	26 ± 1 [*]	36 ± 2 ^{*II}
<i>T₁₂</i>	21 ± 2	19 ± 0 ^{II}	24 ± 1	24 ± 2 ^{II}
<i>T₂₄</i>	19 ± 2	16 ± 1 ^{II}	19 ± 2 ^{II}	20 ± 2 ^{II}
Norepinephrine dose (ug/kg/min)				

<i>Baseline</i>	0.00 ± 0.00	0.00 ± 0.00	0.01 ± 0.01	0.00 ± 0.00
<i>T₀</i>	0.00 ± 0.00	0.01 ± 0.01	0.01 ± 0.01	0.05 ± 0.03
<i>T₃</i>	0.00 ± 0.00	0.12 ± 0.01 ^{*ll}	0.12 ± 0.04 ^{*ll}	0.10 ± 0.03 [*]
<i>T₁₂</i>	0.00 ± 0.00	0.13 ± 0.01 ^{*ll}	0.16 ± 0.03 ^{*ll}	0.15 ± 0.03 ^{*ll}
<i>T₂₄</i>	0.00 ± 0.00	0.24 ± 0.02 ^{*ll}	0.22 ± 0.02 ^{*ll}	0.31 ± 0.04 ^{*‡ll}
Cumulative fluids (L)				
<i>T₂₄</i>	1.6 ± 1.4	3.0 ± 0.3 [*]	3.0 ± 0.4 [*]	3.0 ± 0.6 [*]

Abbreviations: mPAP: mean pulmonary artery pressure; MAP: mean systemic arterial pressure.

* p < 0.05 compared to Sham, † p < 0.05 compared to Non-protective, ‡ p < 0.05 compared to Conventional protective. All time points were compared to T₀. § p < 0.05 for T₀ compared to baseline, ll p < 0.05 compared to T₀.

Table 3. Expression of genes involved in fibroproliferation

Variable	Group		
	Non-protective	Conventional protective	Near-apneic
Pro-Collagen I	1.07 ± 0.46	1.08 ± 0.39	0.99 ± 0.59
Pro-Collagen III	1936 ± 0.83*	1651 ± 0.70*	1838 ± 0.6*
Alpha-SMA	10.40 ± 0.60*	11.85 ± 0.27*	14.13 ± 0.38*
TGF-β1	0.33 ± 0.66	0.34 ± 0.36	0.37 ± 0.58

The $2^{-\Delta\Delta CT}$ values are shown as an estimate of the relative fold expression (in relation to

Sham) of the mRNA in tissue homogenates obtained from the left lung. Abbreviations:

Alpha-SMA: alpha smooth-muscle actin; TGF- β1: transforming growth factor beta 1.

* $p < 0.05$ compared to Sham. No differences were observed between Non-protective, Conventional protective and Near-apneic groups.

Figure 1

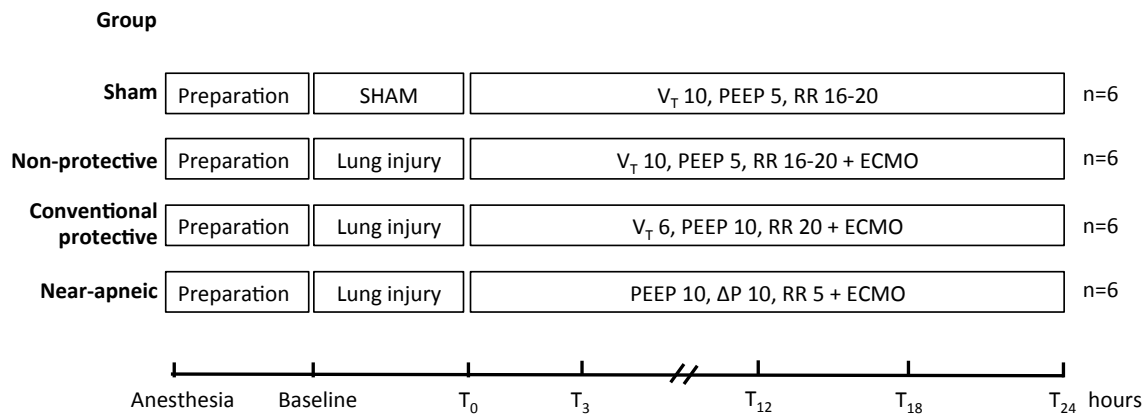


Figure 1. Study design and timeline. Preparation corresponds to anesthesia and invasive monitoring, which took 1-1.5 hours. Lung injury corresponds to the induction of lung injury by 2 hits: repeated saline lavages (1-1.5 hours) followed by 2 hours of injurious ventilation. T₀ to T₂₄ corresponds to the study period, during which each group received a specific ventilatory strategy. Abbreviations: V_T = tidal volume in ml/kg, PEEP = positive end-expiratory pressure in cmH₂O, RR = respiratory rate in breaths/min, ECMO = extracorporeal membrane oxygenation, ΔP = driving pressure in cmH₂O.

Figure 2

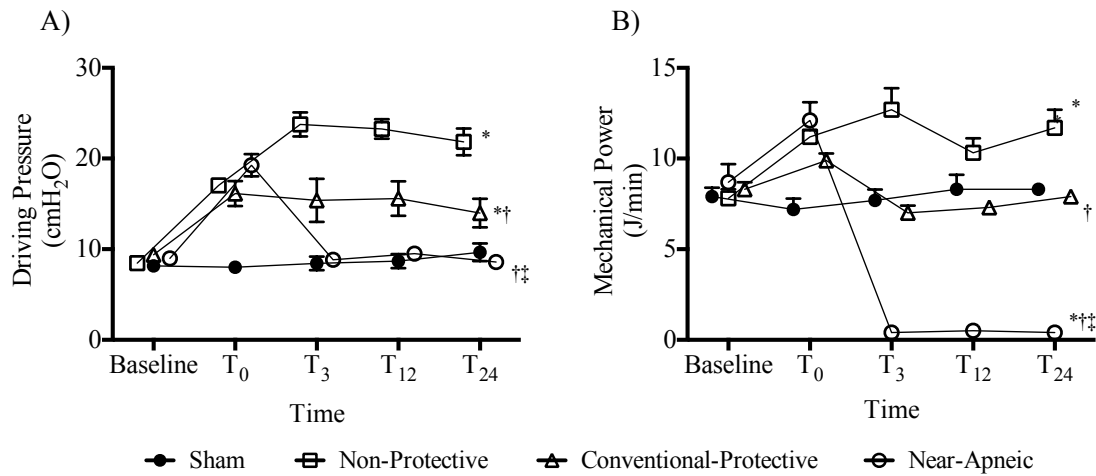
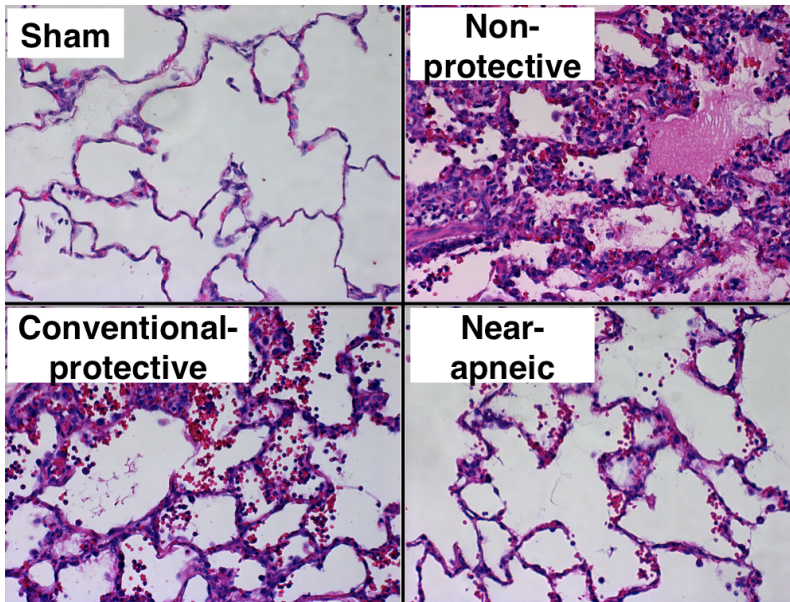


Figure 2. Determinants of VILI. Panel A: Driving pressure, calculated as plateau pressure – PEEP, at different time points for each study group. **Panel B:** Mechanical power, calculated according to Gattinoni et al. (Ref. 17), at different time points for each study group.

* p < 0.05 compared to Sham from T₃ to T₂₄, † p < 0.05 compared to Non-protective from T₃ to T₂₄, ‡ p < 0.05 compared to Conventional protective from T₃ to T₂₄. Only statistical differences between groups are marked.

Figure 3

A



B

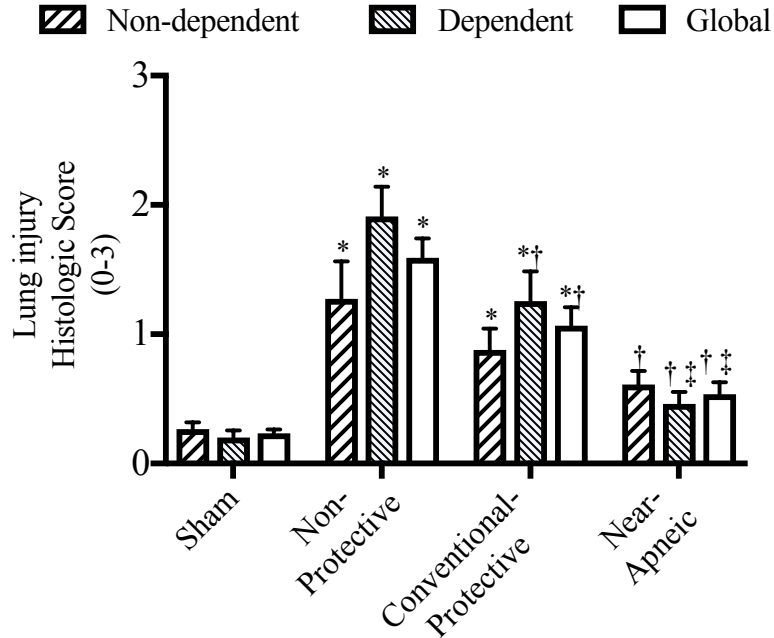


Figure 3. Histological assessment of lung injury. Panel A: Representative images of lung histology for each study group (original magnification: 200x, hematoxylin and eosin).

Images from Non-protective and Conventional protective groups presented diffuse alveolar damage with alveolar edema, hemorrhage, hyaline membranes and inflammatory cells in the interstitium and alveolar spaces; **Panel B:** Quantitative score for lung injury (from 0 = normal, to 3 = maximal alteration), calculated by averaging the scores for alveolar disruption, neutrophil infiltration, and hemorrhage, for dependent and non-dependent areas of the right lung, and the global score (mean of scores for dependent and non-dependent areas).

* $p < 0.05$ compared to Sham; † $p < 0.05$ for differences with Non-protective, ‡ $p < 0.05$ for differences with Conventional protective.

Figure 4

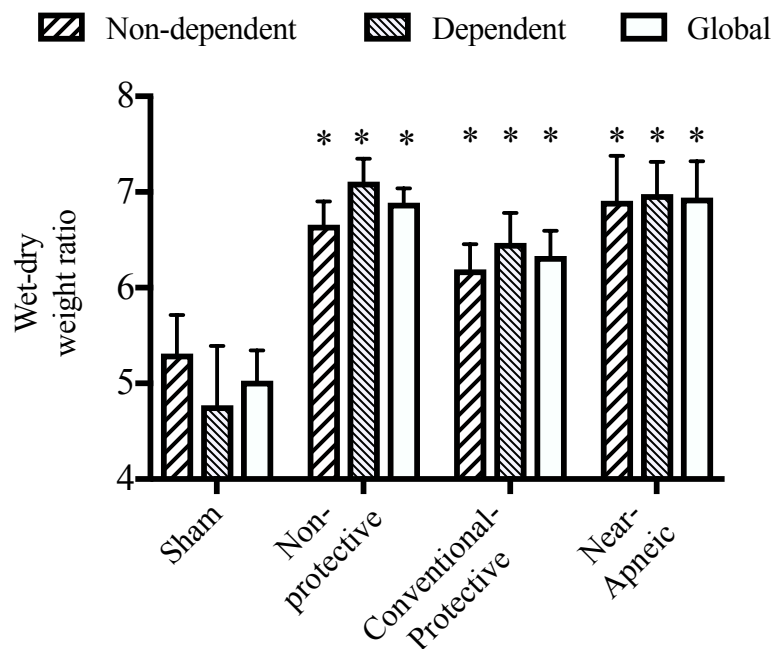
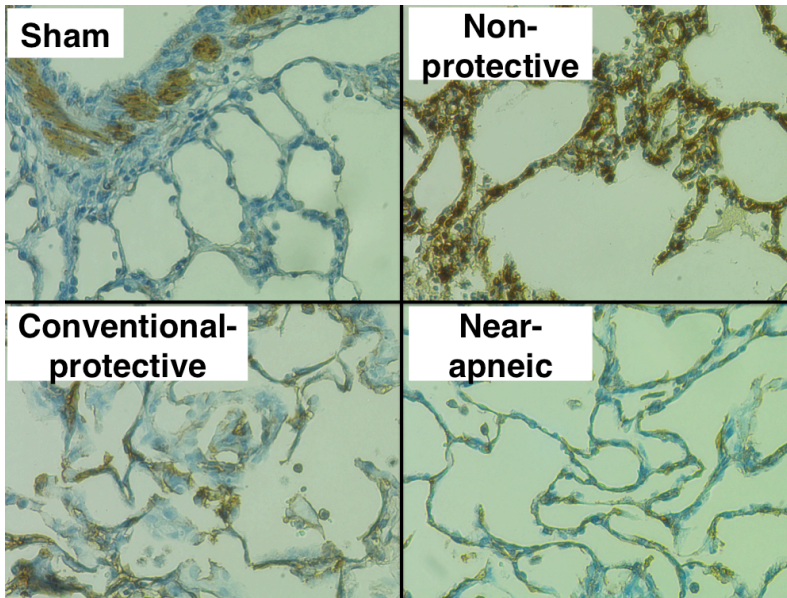


Figure 4. Wet-dry lung weight ratio. Wet-dry weight ratio of dependent and non-dependent areas of the left lung. Global columns correspond to the average of the dependent and non-dependent areas. All injured groups showed a significant increase in their lung water content compared to Sham but no differences were detected between them.

* $p < 0.05$ compared to Sham.

Figure 5

A



B

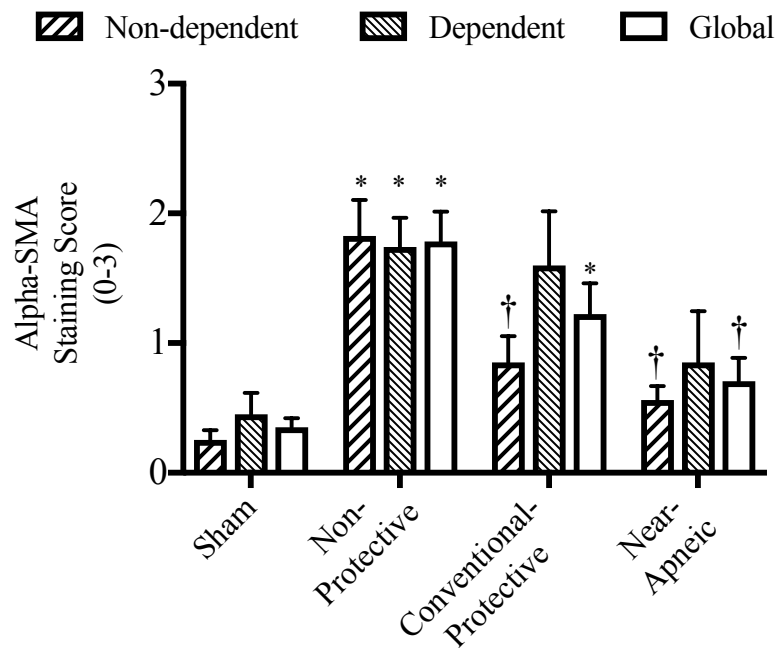


Figure 5. Immunohistochemistry of alpha-SMA. Immunohistochemical staining of alpha-SMA protein as a surrogate for myofibroblasts in lung tissue preparations. **Panel A:**

Representative images for each study group. Brown staining shows a positive reaction for alpha-SMA (original magnification 400x). In the image corresponding to a Sham animal, alpha-SMA staining is limited to the bronchial wall, which usually has a smooth muscle layer. In contrast, the animal from the Non-protective group has extensive staining on its alveolar walls, while the animal from the Conventional protective group exhibits a moderate staining. **Panel B:** Quantitative score for myofibroblast staining (from 0 = no staining, to 3 = maximal staining) for dependent and non-dependent areas of the right lung, and the global score (mean of scores for dependent and non-dependent areas). Staining in bronchial and vascular walls was not considered for scoring.

* $p < 0.05$ compared to Sham; † $p < 0.05$ for differences with Non-protective.

Figure 6

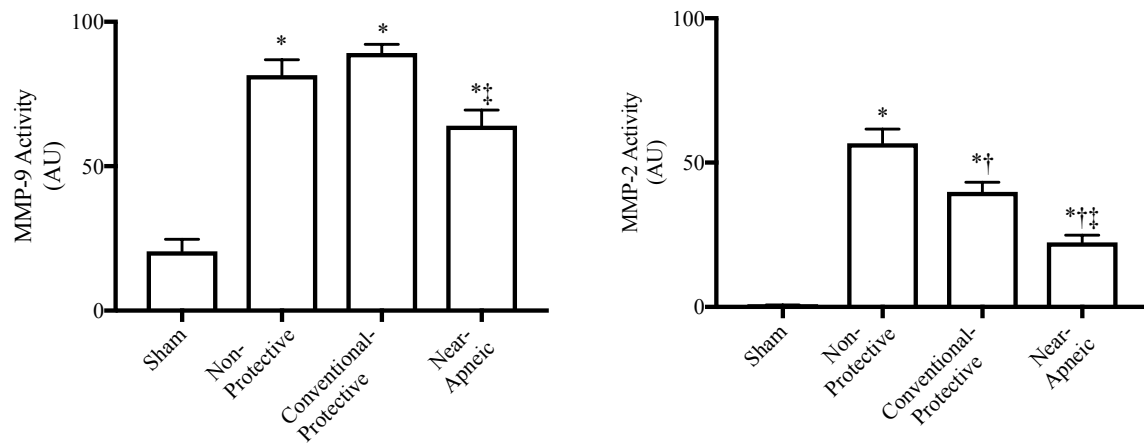


Figure 6. Matrix-metalloproteinase (MMP)-9 and -2 activities in lung tissue.

Quantitative analysis of gelatin zymography performed in homogenates of the left lung. Data is expressed in arbitrary units (AU) of the 90 kDa band, corresponding to the activity of MMP-9 (left), and of the sum of the 68 and 72 kDa bands, corresponding to the activity of MMP-2 (right).

* $p < 0.05$ compared to Sham; † $p < 0.05$ for differences with Non-protective, ‡ $p < 0.05$ for differences with Conventional protective.

Online Data Supplement

Title: “Near-apneic ventilation decreases lung injury and fibroproliferation in an ARDS model with ECMO”

Joaquin Araos; Leyla Alegria; Patricio Garcia; Pablo Cruces; Dagoberto Soto; Benjamín Erranz; Macarena Amthauer; Tatiana Salomon; Tania Medina; Felipe Rodriguez; Pedro Ayala; Gisella R. Borzone; Manuel Meneses; Felipe Damiani; Jaime Retamal; Rodrigo Cornejo; Guillermo Buggedo; Alejandro Bruhn

Appendix 1

Supplementary Methods

The study was approved by the Animal Ethics Committee of Pontificia Universidad Católica de Chile (Protocol 12-029). Animals were treated in accordance with the National Institute of Health's (NIH) guidelines (1). We studied young pigs (3-month-old, weighing 28.6 ± 0.4 kg) of the *Sus scrofa domestica* breed.

Preparation and maintenance

Twenty-four pigs were used in the study. Animals were housed at the research facility the day before, fasted for solid food 12 hours before experiments, with water access *ad libitum*. Animals were pre-medicated with ketamine (20 mg/kg) and xylazine (2 mg/kg) IM. Once sedated, a catheter was placed in the marginal ear vein, and anesthesia induced with a combination of fentanyl (30 ug/kg), midazolam (0.25 mg/kg) and atracurium (0.5 mg/kg) intravenously. Pigs were then intubated with an endotracheal tube (6.5 ID), and connected to a mechanical ventilator (Dräger Evita XL®, Lübeck, Germany) in volume controlled ventilation (VCV) mode. Initial ventilatory settings included positive end-expiratory pressure (PEEP) of 5 cmH₂O, tidal volume (V_T) 10 ml/kg, and an I:E ratio 1:2. Respiratory rate (RR) was initially set at 16-18 min and adjusted thereafter to keep PaCO₂ between 30-50 mmHg. Inspired oxygen fraction (FiO₂) was kept at 1.0 throughout all the experiment. Anesthesia was maintained with a continuous intravenous infusion of a solution consisting of midazolam 2 mg/ml, fentanyl 20 ug/ml and ketamine 20 mg/ml, set at 0.5 ml/kg/h during invasive procedures and induction of lung injury and at 0.25 ml/kg/h thereafter until the end of the experiment. Depth of anesthesia was assessed regularly by checking for movements

and hemodynamic response to a painful stimulus. Muscle paralysis was then maintained with a continuous infusion of atracurium (0.5 mg/kg/h) throughout the experiment. At the time of instrumentation a dose of 30 mg/kg of cephazolin was administered intravenously and repeated every 8 hours thereafter. Body temperature of the animals was kept at $38 \pm 1^\circ\text{C}$.

Under sterile conditions, the left carotid artery and left external jugular vein were surgically exposed for insertion of arterial and pulmonary artery catheters, respectively. A pulmonary artery catheter was placed under direct pressure curve guidance. After completing instrumentation, baseline data was collected. Electrocardiogram, arterial blood pressure, pulmonary artery pressure, heart rate, pulse oximetry, and core temperature were monitored periodically.

Animals received normal saline at 10 ml/kg/h during preparation and while inducing lung injury, and 2 ml/kg/h during the 24-hour study period. In pilot experiments we observed that hypotension was frequent after connection to ECMO, and that moderate doses of noradrenaline were required despite adequate fluid loading. Therefore, our protocol established that a noradrenaline infusion was started promptly after connection to ECMO in case mean arterial pressure fell below 65 mmHg. If hypotension persisted despite noradrenaline (0.1 ug/kg/min), animals received a fluid challenge with normal saline 2 ml/kg. Further fluid challenges were decided according to fluid and vasopressor responsiveness.

After baseline measurements animals were allocated to Sham (n=6) or lung injury (n=18).

Induction of lung injury

A 2-hit model of ARDS was applied, starting with lung lavages to deplete the lungs of

alveolar surfactant, followed by injurious mechanical ventilation. With animals under deep anesthesia and fully monitored, repeated lung lavages with warm saline (30 ml/kg, 39°C) were performed, alternating 2 in supine and 2 in prone position. The setting of mechanical ventilation between lavages was the same as that described above. Subsequent lavages were performed if necessary until $\text{PaO}_2/\text{FiO}_2$ fell below 250 mmHg for at least 15 minutes while in supine position. Subsequently, a two-hour period of injurious ventilation was started in pressure control ventilation, with PEEP 0 cmH₂O and inspiratory pressure of 40 cmH₂O, at a respiratory rate of 10/min, an I:E of 1:1, and FiO_2 1.0. The first hour was in prone position and the second in supine position. After completing this two-hour period, ventilator settings were returned back to those used at baseline, and after 10 minutes, before starting ECMO, a full assessment of all variables was registered (time 0, abbreviated as T₀).

Extracorporeal membrane oxygenation (ECMO) support

The ECMO equipment included a magnetic Medtronic Bio-Medicus® 540 centrifugal pump (Eden Prairie, MN, USA), a coagulation monitor (Hemochron® Response, ITC, USA), and a heat exchanger HU-35 (Maquet, USA). The circuit comprised a HILITE® 2400LT polymethylpentene hollow fiber membrane oxygenator, 0.65 m² (MEDOS, Stolberg, Germany), polyvinyl chloride 1/4-inch lines coated with heparin, and a Rotaflow 32 head pump (Maquet, USA). The circuit was primed with saline. Pressure transducers were placed before and after the membrane, and a negative pressure transducer was connected to the drainage line.

In animals from the lung injury groups cannulation was performed during the second hour of injurious ventilation, with pigs in the supine position. Under sterile conditions, the right

external jugular vein was surgically exposed and a 23-F bi-caval dual lumen (BCDL) cannula (AVALON ELITE®, Maquet, USA) was inserted and directed towards the inferior vena cava, and secured at 18 cm from the tip. In pilot experiments we observed that the infusion port consistently remained facing the right atrium at this depth. Anticoagulation was induced with an intravenous heparin bolus (100 IU/kg), followed by a continuous infusion targeting an activated clotting time (ACT) of 180–220s. The BCDL cannula was connected to the circuit after T_0 measurements and extracorporeal circulation started progressively. The pump was adjusted to target a blood flow > 65 ml/kg/min, but keeping pressure in the drainage line above -70 mmHg. Heat exchanger was set at 38 °C. The initial sweep gas flow (FiO_2 1.0) was set at 1:1 with blood flow, and then titrated to keep an arterial $PaCO_2$ between 40 ± 10 mmHg.

After T_0 measurements, the 18 animals with lung injury were randomly allocated to one of three groups (Non-protective, Conventional protective, or Near-apneic). The ventilatory protocol was gradually implemented during the first 30 minutes of ECMO run to avoid hemodynamic instability.

Sham animals received neither lung injury nor ECMO. Instead, they underwent a 3-hour stabilization period between baseline and T_0 measurements to keep a parallel time line.

Ventilatory protocol during the 24-hour study period, according to study group

- Sham: volume control ventilation (VCV), V_T 10 ml/kg, PEEP 5 cmH₂O, RR as baseline, I:E ratio 1:2 (n = 6).
- Non-protective: volume control ventilation (VCV), V_T 10 ml/kg, PEEP 5 cmH₂O,

RR as baseline, I:E ratio 1:2 (n = 6).

- Conventional protective: volume control ventilation (VCV), V_T 6 ml/kg, PEEP 10 cmH₂O, RR 20 bpm, I:E ratio 1:2 (n = 6).
- Near-apneic: pressure control ventilation, starting with PEEP 10 cmH₂O + driving pressure 10 cmH₂O, RR 5 bpm, at an I:E ratio of 1:1. If $V_T > 2$ ml/kg, PEEP was increased while decreasing driving pressure, until $V_T \leq 2$ ml/kg, keeping mean airway pressure stable at 15 cmH₂O (n = 6).

Physiological measurements and sample collection

Heart rate, pulse oximetry, core temperature, arterial blood pressure, pulmonary artery pressure, respiratory rate and respiratory mechanics, ventilator and ECMO settings, anesthetic drugs and maintenance fluid as well as infusion drugs for hemodynamic support were recorded and registered hourly for the 24-hour study period. Driving pressure was calculated as the difference between end-inspiratory pressure at 0 flow (plateau pressure) minus PEEP (2). Mechanical power was calculated using the program Energy Calculator Software (University of Gottingen, Germany) (3).

Blood was drawn for arterial and mixed venous blood gas analysis and for obtaining plasma samples at baseline (after anesthesia induction and catheterization), at T_0 , and after 3, 12 and 24 hours (T_3 , T_{12} and T_{24}). Plasma was obtained by centrifugation of blood samples at 2000 g for 10 minutes. These samples were immediately frozen and kept at -80° C for future analysis.

At the end of the 24-hour study period, animals were euthanized by an overdose of thiopental and T-61 solution IV(4). Immediately after euthanasia, a thoracotomy was performed in order to access the lungs. Lungs were kept at a pressure of 20 cmH₂O by application of an inspiratory pause and clamping the ET tube thereafter. The left bronchus was then tightly sutured in order to separate the left from the right lung. A transversal lung slice was cut at the middle region of the left lung (midway between cranial and caudal regions). Samples were obtained from dependent and non-dependent areas of the slice for the estimation of lung water accumulation and for further determinations (snap-frozen with liquid nitrogen and kept at -80° C). The right lung was filled with formaldehyde at 20 cmH₂O and the trachea clamped to avoid formaldehyde losses. After 24 hours of fixation a transversal lung slice was cut at the middle region of the right lung and samples were obtained from dependent and non-dependent areas and embedded in paraffin.

Histological analysis

To assess lung injury, tissue slices were cut from paraffin blocks, stained with hematoxylin and eosin, and observed with light microscopy. A validated score (5) was used to evaluate 3 parameters of lung injury: alveolar disruption, neutrophil infiltration and hemorrhage; each of these categories received a score ranging from 0 to 3, where 0 corresponds to no pathologic alteration, 1 corresponds to mild, 2 corresponds to moderate and 3 corresponds to severe pathologic alteration. Twenty random areas were evaluated for each section at 200x magnification and its values averaged.

To determine the presence of active myofibroblasts and pro-collagen III in lung tissue, the abundance of alpha-smooth muscle actin (SMA) positive cells, and pro-collagen III positive tissue was evaluated using immunohistochemistry by the immunoperoxidase technique.

Endogenous peroxidase activity in lung sections was blocked with 3% H₂O₂ for 10 min. Non-specific reactivity was then blocked with horse-serum reactive for 10 min. Thereafter, for alpha SMA, samples were incubated with a mouse (with reactivity for pigs) monoclonal anti-alpha-SMA antibody (1:250) for 40 minutes at 37°C (Millipore-Sigma, Darmstadt, Germany). And for pro-collagen III, samples were incubated with mouse monoclonal antibody against pro-collagen alpha 1, type III of human origin (Santa Cruz Biotechnology, Texas, USA) for 40 minutes at 37°C. This antibody also has cross-reaction with the porcine species. A 1:200 dilution was used. After repeated washing with PBS, samples were incubated with rabbit biotinylated secondary antibody anti-mouse IgG for 25 min at 37°C. This process was followed by avidin-biotin amplification for 25 min and incubation with 3'-3' diaminobenzidine for 2 min at room temperature. Nuclear counterstain using Harris hematoxylin for 1 min was followed by graded sequential dehydration in ethanol. A semi-quantitative score was used to evaluate the staining on histological preparations. Briefly, 20 random fields (200X) were evaluated and a score ranging from 0-3 (where 0 corresponds to no staining, 1 corresponds to mild, 2 corresponds to moderate and 3 corresponds to extensive staining) was given to each field, and then an average obtained. Staining of bronchial and vessel walls was not considered for these scores because these structures normally have alpha SMA and pro-collagen III.

A blinded, board certified pathologist (M.M.) performed all histological assessments. Results are reported for the dependent, non-dependent and global (averaged dependent and non-dependent) areas.

Wet / dry lung weight ratio

In order to estimate changes in lung water accumulation, the wet / dry weight ratio was obtained (6). Lung sections from dependent and non-dependent areas of the middle region of the left lung were weighted before and after drying them for 24 hours in an oven at 120° C.

Lung tissue levels of transforming growth factor- β 1 (TGF- β 1)

A commercially available ELISA kit (R&D Systems Inc., Minneapolis, MN, USA) was used to evaluate TGF- β 1 levels in lung tissue homogenates from the middle region of the left lung. Manufacturer instructions were followed.

Messenger RNA expression of genes associated with fibroproliferation

A PCR array specifically designed for pigs (Qiagen, Hilden, Germany) was used to determine the expression of 4 relevant genes involved in fibroproliferative processes in lung tissue samples, including collagens I and III, alpha-SMA and TGF- β 1 in the left middle lung region. Briefly, total RNA was obtained from lung tissue previously kept at -80°C, using the RNeasy Microarray Tissue Mini Kit, following manufacturer instructions. cDNA from purified RNA was then obtained using the RT2 First Strand Kit. cDNA was then added to the RT2 SYBR Green Mastermix and then aliquots were mixed into the RT2 Profiler PCR Array containing the genes of interest. Arrays were read using an ABI 7500 real-time PCR system (Life Technologies). GAPDH was used as housekeeping gene. Relative real-time RT-PCR quantitation was performed according to Livak and Schmittgen (7), using the comparative threshold cycle (CT) values (8). Delta-delta C_T ($\Delta\Delta$ CT) was calculated as follows:

$$\Delta\Delta C_T = (C_{T,Target} - C_{T,GAPDH})_{Injured} - (C_{T,Target} - C_{T,GAPDH})_{Sham\ group},$$

where $(C_{T,Target} - C_{T,GAPDH})_{Sham}$ represents normalized expression in Sham, and $(C_{T,Target} - C_{T,GAPDH})_{Injured}$ is the normalized expression for each injured group. The relative fold expression (RFE) of the target genes was calculated as follows:

$$RFE = 2^{-\Delta\Delta C_T},$$

Results were analyzed and compared between groups with the relative expression software tool (REST ©) (9).

Matrix-metalloproteinase (MMP) 2 and 9 activity

MMP-2 and 9 gelatinolytic activities in lung tissue homogenate (left middle lung region) were measured by gelatin zymography. Briefly, 30 μ g of total protein in lung homogenate supernatant were placed into a gelatin-containing electrophoresis gel (10% polyacrylamide and 1% gelatin under non-reducing conditions). After electrophoresis, gels were washed in 2.5% Triton X-100 to remove SDS, incubated over night at 37°C with a developing buffer (10) and stained with 0.1% Coomassie brilliant blue. Densitometric analysis was performed using Image J 1.47v (NIH, Bethesda, MD). The resolution of gels consistently provided 1 gelatinolytic band for MMP-9 (approximately 90 kDa) and 2 bands for MMP-2 (approximately 68 and 72 kDa); consequently, MMP-9 activity is reported as the single gelatinolytic 90 kDa band density whereas MMP-2 activity is reported as the sum of the 2-

gelatinolytic band densities (68 and 72 kDa). The results of 4 gels developed under similar conditions were averaged and reported accordingly.

Statistical analysis

Statistical analysis was performed with GraphPad Prism 7 (GraphPad Software, USA). Data measured along time were analyzed using repeated measures two-way ANOVA, followed by Tukey's multiple comparisons test, both for differences between groups (all groups compared with each other) and along time (all time points compared to T₀). Data derived from lung tissue analysis was compared with one-way ANOVA, followed by Tukey's multiple comparisons test. Association between variables was analyzed by linear regression. Statistical significance was set at $p < 0.05$. Data are expressed as mean \pm standard error of the mean.

REFERENCES

- E1. Institute for Laboratory Animal Research. *Guide for the Care and Use of Laboratory Animals: 8th Ed. Guid Care Use Lab Anim* 2011. doi:10.2307/1525495.
- E2. Amato MBP, Meade MO, Slutsky AS, Brochard L, Costa ELV, Schoenfeld DA, Stewart TE, Briel M, Talmor D, Mercat A, Richard J-CM, Carvalho CRR, Brower RG. Driving Pressure and Survival in the Acute Respiratory Distress Syndrome. *N Engl J Med* 2015;372:747–755.
- E3. Gattinoni L, Tonetti T, Cressoni M, Cadringer P, Herrmann P, Moerer O, Protti A, Gotti M, Chiurazzi C, Carlesso E, Chiumello D, Quintel M. Ventilator-related causes of lung injury: the mechanical power. *Intensive Care Med* 2016;42:1567–1575.

- E4. Leary S, Underwood W, Anthony R, Cartner S. *AVMA Guidelines for the Euthanasia of Animals: 2013 Edition*. *Am Vet Med Assoc* 2013. doi:10.1016/B978-012088449-0.50009-1.
- E5. Retamal J, Bergamini B, Carvalho AR, Bozza FA, Borzone G, Borges J, Larsson A, Hedenstierna G, Bugedo G, Bruhn A. Non-lobar atelectasis generates inflammation and structural alveolar injury in the surrounding healthy tissue during mechanical ventilation. *Crit Care* 2014;18:505.
- E6. Matsuyama H, Amaya F, Hashimoto S, Ueno H, Beppu S, Mizuta M, Shime N, Ishizaka A, Hashimoto S. Acute lung inflammation and ventilator-induced lung injury caused by ATP via the P2Y receptors : an experimental study. 2008;13:1–13.
- E7. Livak KJ, Schmittgen TD. Analysis of relative gene expression data using real-time quantitative PCR and. *Methods* 2001;25:402–408.
- E8. Pfaffl MW. A new mathematical model for relative quantification in real-time RT-PCR. *Nucleic Acids Res* 2001;29:45e–45.
- E9. Pfaffl MW, Horgan GW, Dempfle L. Relative expression software tool (REST) for group-wise comparison and statistical analysis of relative expression results in real-time PCR. *Nucleic Acids Res* 2002;30:e36.
- E10. Toth M, Sohail A, Fridman R. Assessment of gelatinases (MMP-2 and MMP-9) by gelatin zymography. *Methods Mol Biol* 2012;878:121–135.

Appendix 2

Supplementary Tables

Table E1. ECMO settings

Variable	Time	Group		
		Non-protective	Conventional protective	Near-apneic
Sweep gas flow (L/min)	T_1	0.8 ± 0.2	1.1 ± 0.2	$3.4 \pm 0.5^{\dagger\ddagger}$
	T_{24}	0.7 ± 0.1	1.5 ± 0.3	$3.1 \pm 0.4^{\dagger\ddagger}$
Pump speed (RPM)	T_1	2670 ± 340	2911 ± 273	3140 ± 275
	T_{24}	2825 ± 165	2778 ± 226	3142 ± 276
Blood flow (L/min)	T_1	1.7 ± 0.3	1.7 ± 0.1	2.0 ± 0.2
	T_{24}	2.0 ± 0.3	1.6 ± 0.1	2.1 ± 0.2
Trans P (mmHg)	T_1	22 ± 2	30 ± 3	31 ± 6
	T_{24}	33 ± 1	30 ± 4	27 ± 6
ACT (seconds)	T_1	154 ± 20	189 ± 30	173 ± 25
	T_{24}	213 ± 1	192 ± 20	203 ± 10

Abbreviations: RPM: revolutions per minute, Trans P: transmembrane pressure, ACT:

activated clotting time. T_1 : Time 1 hour after starting the study period. T_{24} : Time 24 hours after starting the study period.

† $p < 0.05$ compared to Non-protective, ‡ $p < 0.05$ compared to Conventional protective.

Table E2. Biochemical variables

Variable	Group			
	Sham	Non-protective	Conventional protective	Near-apneic
Time				
Creatinine (mg/dl)				
<i>Baseline</i>	1.0 ± 0.2	0.9 ± 0.0	0.8 ± 0.1	0.7 ± 0.1
<i>T₀</i>	1.0 ± 0.2	1.0 ± 0.1	0.7 ± 0.1	0.8 ± 0.1
<i>T₁₂</i>	1.1 ± 0.1	1.6 ± 0.4	0.9 ± 0.1 [†]	1.1 ± 0.1
<i>T₂₄</i>	1.1 ± 0.3	1.8 ± 0.3 ^{* II}	1.3 ± 0.1	1.2 ± 0.2
BUN (mg/dl)				
<i>Baseline</i>	10.2 ± 2.7	8.8 ± 0.5	11.4 ± 1.3	11.5 ± 1.1
<i>T₀</i>	10.2 ± 2.3	7.8 ± 0.5	12.2 ± 2.3	11 ± 1.7
<i>T₁₂</i>	19.0 ± 5.1	17.3 ± 1.4	18.2 ± 1.5	17.5 ± 1.5
<i>T₂₄</i>	18.3 ± 6.9	22.2 ± 3.0 ^{II}	23.2 ± 2.2 ^{II}	19.5 ± 0.9
AST (U/L)				
<i>Baseline</i>	49 ± 5	23 ± 4	38 ± 7	32 ± 5
<i>T₀</i>	60 ± 4	37 ± 14	53 ± 10	48 ± 9
<i>T₁₂</i>	96 ± 17	91 ± 26 ^{II}	32 ± 11 ^{*†}	59 ± 7
<i>T₂₄</i>	102 ± 22	134 ± 32 ^{II}	72 ± 10 [†]	64 ± 11 [†]
Bilirubin (mg/dl)				
<i>Baseline</i>	0.2 ± 0.0	0.2 ± 0.0	0.2 ± 0.0	0.2 ± 0.0
<i>T₀</i>	0.2 ± 0.1	0.2 ± 0.0	0.2 ± 0.0	0.2 ± 0.0
<i>T₁₂</i>	0.2 ± 0.0	0.2 ± 0.0	0.2 ± 0.0	0.2 ± 0.0

T_{24}	0.2 ± 0.0	0.2 ± 0.0	0.2 ± 0.0	0.2 ± 0.0
pH				
<i>Baseline</i>	7.51 ± 0.03	7.49 ± 0.33	7.55 ± 0.02	7.50 ± 0.03
T_0	7.51 ± 0.03	7.41 ± 0.04	7.48 ± 0.03	7.40 ± 0.03
T_{12}	7.38 ± 0.02	7.47 ± 0.02	7.33 ± 0.02	7.36 ± 0.03
T_{24}	7.42 ± 0.03	7.43 ± 0.02	7.36 ± 0.02	7.37 ± 0.03
HCO₃⁻ (mEq/L)				
<i>Baseline</i>	30.6 ± 1.0	31.2 ± 0.9	31.0 ± 1.1	33.0 ± 1.1
T_0	29.8 ± 0.7	$25.3 \pm 1.4^{*\$}$	$21.9 \pm 1.0^{*\$}$	$23.5 \pm 0.8^{*\$}$
T_{12}	25.9 ± 1.1	24.7 ± 1.0	24.0 ± 1.0	25.2 ± 1.4
T_{24}	24.3 ± 1.9^{II}	23.9 ± 0.8	23.0 ± 1.4	25.5 ± 2.0
Base Excess (mEq/L)				
<i>Baseline</i>	7.5 ± 1.6	8.5 ± 1.3	8.7 ± 1.1	9.5 ± 1.2
T_0	6.5 ± 1.1	$2.8 \pm 1.5^{\$}$	$1.0 \pm 1.3^{*\$}$	$0.3 \pm 0.7^{*\$}$
T_{12}	2.3 ± 0.7^{II}	2.0 ± 0.8	1.5 ± 2.6	2.5 ± 0.9
T_{24}	4.3 ± 0.9	1.5 ± 0.5	0.5 ± 1.2	3.2 ± 1.5
Lactate (mmol/L)				
<i>Baseline</i>	1.5 ± 1.4	1.5 ± 1.1	1.5 ± 1.1	1.1 ± 0.3
T_0	1.7 ± 0.3	3.1 ± 0.3	2.4 ± 0.3	1.6 ± 0.2
T_{12}	2.0 ± 0.3	1.5 ± 0.1	1.1 ± 0.1	1.1 ± 0.1
T_{24}	1.4 ± 0.2	1.4 ± 0.3	1.2 ± 0.1	1.0 ± 0.8

Abbreviations: T_0 , T_{12} and T_{24} : times 0, 12 and 24 hours of the study period; BUN: blood urea nitrogen; AST: aspartate aminotransferase; HCO₃⁻: bicarbonate.

* $p < 0.05$ compared to Sham, † $p < 0.05$ compared to Non-protective. All time points were compared to T_0 . § $p < 0.05$ for T_0 compared to baseline, †† $p < 0.05$ compared to T_0 .

Table E3. Histological parameters of lung injury

	Group			
	Sham	Non-protective	Conventional protective	Near-apneic
<i>Dependent</i>				
Alveolar disruption	0.1 ± 0.0	1.2 ± 0.1*	0.8 ± 0.2*	0.3 ± 0.1†‡
Neutrophil infiltration	0.1 ± 0.0	2.3 ± 0.3*	1.7 ± 0.2*†	0.7 ± 0.2†
Hemorrhage	0.4 ± 0.2	2.2 ± 0.4*	1.2 ± 0.4	0.4 ± 0.1†‡
<i>Non-dependent</i>				
Alveolar disruption	0.0 ± 0.0	0.9 ± 0.3*	1.0 ± 0.2*	0.7 ± 0.2
Neutrophil infiltration	0.3 ± 0.2	1.4 ± 0.3*	1.0 ± 0.3*	0.7 ± 0.2†
Hemorrhage	0.5 ± 0.1	1.5 ± 0.3*	0.8 ± 0.2*	0.6 ± 0.2†

Values correspond to scores for alveolar disruption, neutrophil infiltration and hemorrhage (from 0 = normal, to 3 = maximal alteration), in dependent and non-dependent areas of the right lung.

* $p < 0.05$ compared to Sham, † $p < 0.05$ compared to Non-protective, ‡ $p < 0.05$ compared to Conventional protective.

Appendix 3

Supplementary Figures

Figure E1

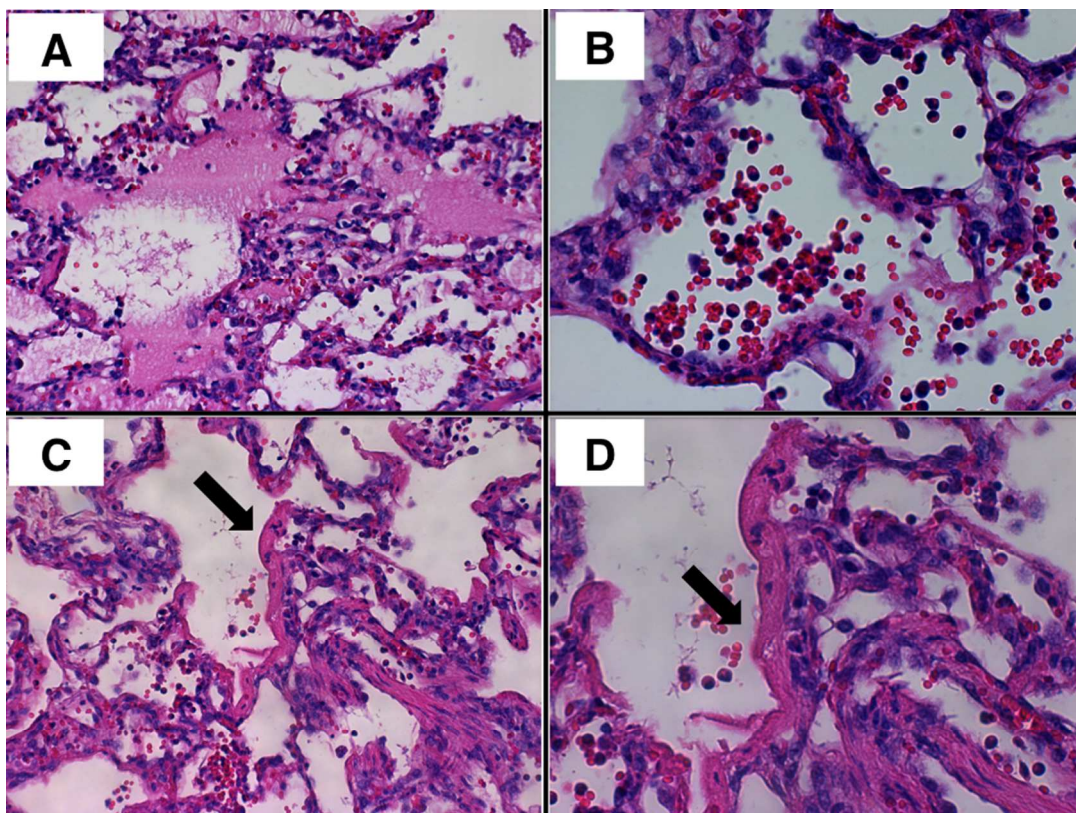
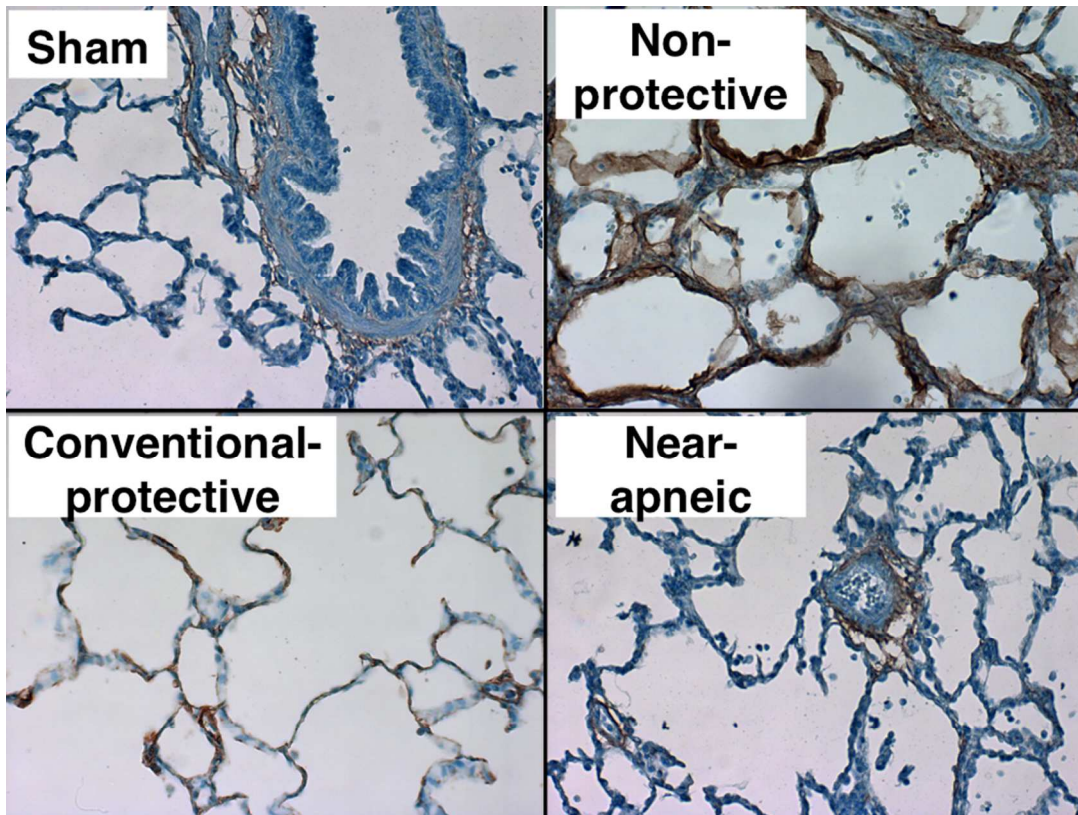


Figure E1. Representative histological images of diffuse alveolar damage.

Representative histologic images of lung tissue from animals subjected to lung injury are shown. All injured groups showed evidence of diffuse alveolar damage although the magnitude and frequency of findings differed between them. **Panel A:** loss of alveolar architecture with presence of abundant alveolar edema (magnification 200x); **Panel B:** marked alveolar infiltrate of erythrocytes and neutrophils (400x); **Panel C:** thick hyaline membranes (black arrow) deposited in the alveolar wall (200x); **Panel D:** a closer magnification of the hyaline membrane shown in Panel C (400x).

Figure E2

A



B

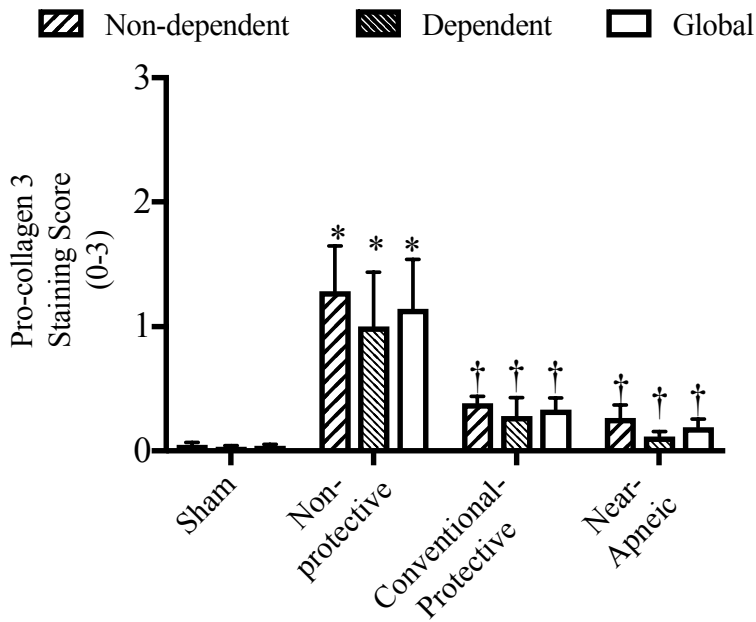
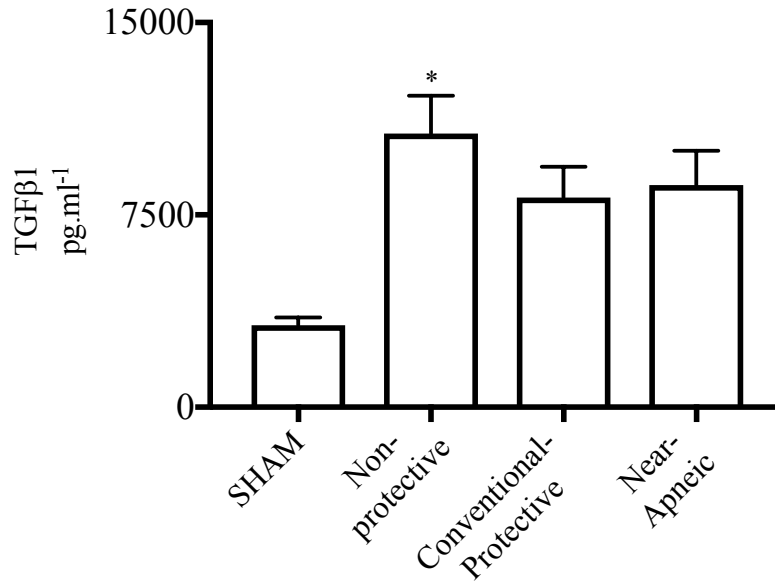


Figure E2. Immunohistochemistry of pro-collagen III. Panel A: Representative images for each study group. Brown staining shows a positive reaction for pro-collagen III (original magnification 400x). In the image corresponding to a Sham animal, pro-collagen III staining is limited to the bronchial wall, which usually has a smooth muscle layer. In contrast, the animal from the Non-protective group has extensive staining on its alveolar walls. **Panel B:** Quantitative score for pro-collagen 3 staining (from 0 = no staining, to 3 = maximal staining). Staining in bronchial and vascular walls was not considered for scoring.

* $p < 0.05$ compared to Sham; † $p < 0.05$ for differences with Non-protective.

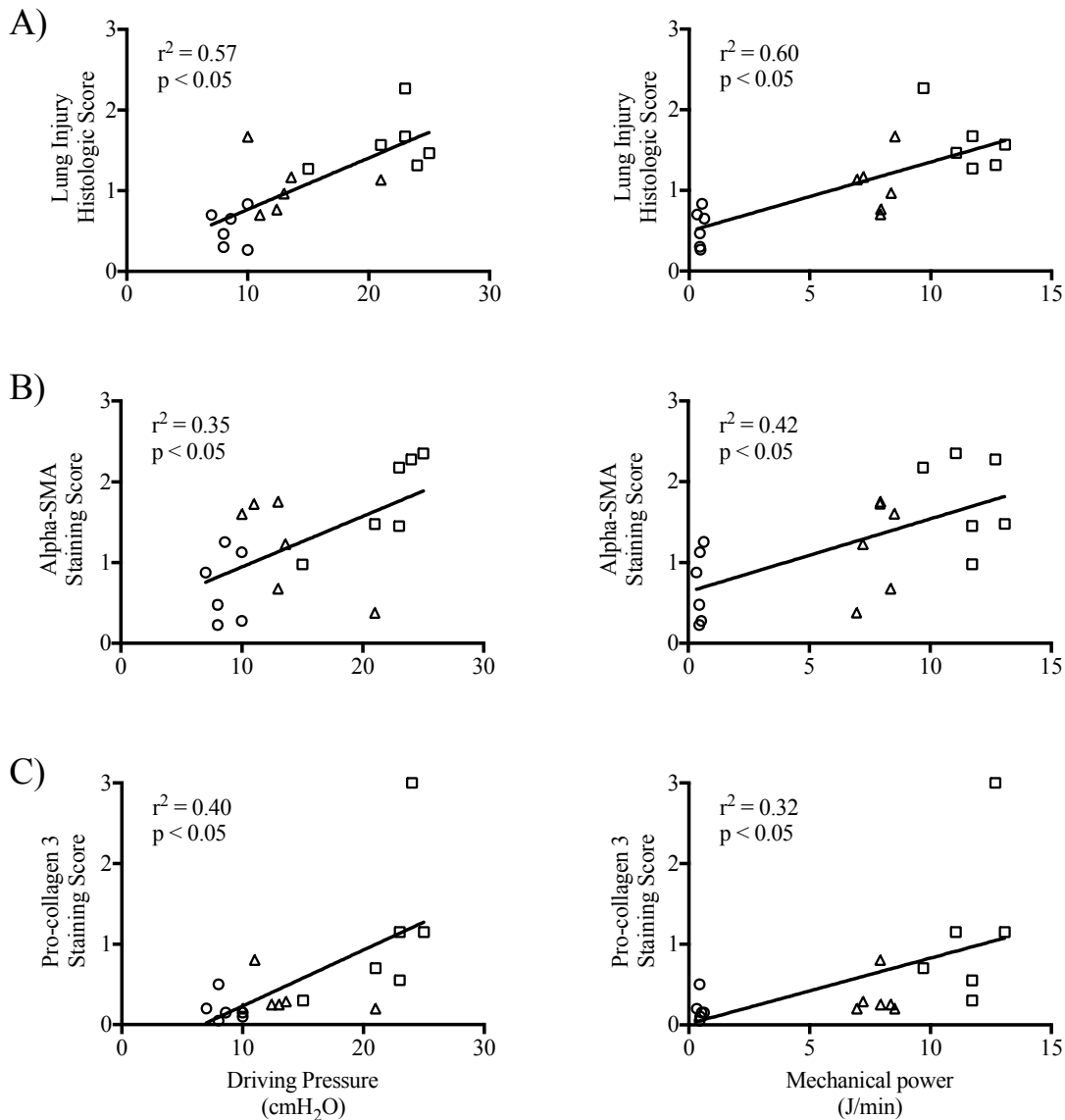
Figure E3

**Figure E3. TGF-β1 concentrations in lung tissue.**

TGF-β1 concentrations in homogenates of tissue obtained from the left lung were analyzed by ELISA.

* $p < 0.05$ compared to Sham.

Figure E4

**Figure E4. Correlations between histological scores and VILI determinants.**

Panel A: Correlation of Lung injury histologic score with driving pressure (left) and mechanical power (right). **Panel B:** Correlation of Alpha SMA staining score with driving pressure (left) and mechanical power (right). **Panel C:** Correlation of Pro-collagen II staining score with driving pressure (left) and mechanical power (right). Squares represent animals from Non-protective, triangles from Conventional protective, and circles from

Near-apneic group. Values of r^2 were obtained with linear regression analysis. $p < 0.05$ represents significant deviance from zero.